Department of Materials Science and Engineering

Developing a Thermodynamic Database for Lead-Based Alloys

Iina Vaajamo

Aalto University

DOCTORAL DISSERTATIONS

Aalto University publication series
DOCTORAL DISSERTATIONS 173/2013

Developing a Thermodynamic Database for Lead-Based Alloys

Iina Vaajamo

A doctoral dissertation completed for the degree of Doctor of Science in Technology to be defended, with the permission of the Aalto University School of Chemical Technology, at a public examination held at the lecture hall V1 of the school on 15 November 2013 at 12.

Aalto University
School of Chemical Technology
Department of Materials Science and Engineering
Metallurgical Thermodynamics and Modelling

Supervising professor
Professor Pekka Taskinen

Thesis advisor
Professor Pekka Taskinen

Preliminary examiners
Professor Luís Filipe Malheiros de Freitas Ferreira, Porto University, Portugal
Doctor Yanping Xiao, Tata Steel RD&T, The Netherlands

Opponent
Professor Jan Vřešťál, Masaryk University, Czech Republic

Aalto University publication series
DOCTORAL DISSERTATIONS 173/2013

ISBN 978-952-60-5401-8
ISBN 978-952-60-5402-5 (pdf)
ISSN-L 1799-4934
ISSN 1799-4934 (printed)
ISSN 1799-4942 (pdf)
http://urn.fi/URN:ISBN:978-952-60-5402-5

Images: "Equilibrium" by Iina Vaajamo (cover)

Unigrafia Oy
Helsinki 2013

Finland

441 697
Printed matter

Aalto University

Abstract

Aalto University, P.O. Box 11000, FI-00076 Aalto www.aalto.fi

Author
Iina Vaajamo

Name of the doctoral dissertation
Developing a Thermodynamic Database for Lead-Based Alloys

Publisher School of Chemical Technology

Unit Department of Materials Science and Engineering

Series Aalto University publication series DOCTORAL DISSERTATIONS 173/2013

Field of research Metallurgy

Manuscript submitted 9 August 2013 **Date of the defence** 15 November 2013

Permission to publish granted (date) 8 October 2013 **Language** English

☐ **Monograph** ☒ **Article dissertation (summary + original articles)**

Abstract

The availability of advanced thermodynamic databases and software and the CALPHAD method allow different phenomena, i.e. phase transformations, and chemical reactions, to be evaluated mathematically by means of thermodynamic calculations. These calculations require internally consistent and reliable thermodynamic databases, such as the MTOX (metal-oxide-sulphide-fluoride) database. MTOX covers the thermodynamic data of the systems related to metal smelting and refining processes, where lead is often considered as an impurity coming from the primary and secondary raw materials. Better knowledge of the thermodynamic behaviour of lead and its alloys can help in developing the smelting, refining and slag cleaning processes where lead often exists as a component.

In this thesis, the mutual solubilities of molten lead and solid metallic foils (Ni, Fe, Cu, Fe-Ni) were measured by means of an isothermal equilibration technique at elevated temperatures, in specially formed quartz ampoules. The chemical compositions of the saturated metals were analysed with an ICP spectrometer and by EPMA.

Literature surveys of the experimental data of the respective systems were performed with the aim of covering all the published data from the early 20th century until today.

The critically evaluated and selected experimental literature data together with the data obtained from my own experiments were used to optimize the thermodynamic interaction parameters of the solution phases with the CALPHAD method. These phases were described in terms of a simple substitutional solution model. For the pure elements the SGTE Unary data were used. The systems were assessed with MTDATA software and the experimental data were fitted by a least square method.

The new experimental data obtained within this thesis enabled the determination of more accurate thermodynamic description of the present systems. In particular, the lead solid solubility in the solid metals, below the monotectic temperature, had not been determined experimentally before with this accuracy. The metal solubilities in molten lead of these systems are rather well known and are in agreement with the results obtained in this thesis.

The thermodynamic description of the Ni-Pb, Fe-Pb, Cu-Pb and Fe-Ni-Pb systems have been improved/established. The overall agreement of the calculated phase diagrams with the critically selected experimental data is good. The thermodynamic assessment of these lead-alloy systems can be used together with the MTOX database to calculate the thermodynamic properties and phase equilibria of multicomponent systems and consequently, to solve practical problems related to materials engineering and metallurgy.

Keywords Thermodynamics, CALPHAD, Equilibration experiment, Solubility, MTOX, Database, Lead

ISBN (printed) 978-952-60-5401-8 **ISBN (pdf)** 978-952-60-5402-5

ISSN-L 1799-4934 **ISSN (printed)** 1799-4934 **ISSN (pdf)** 1799-4942

Location of publisher Helsinki **Location of printing** Helsinki **Year** 2013

Pages 110 **urn** http://urn.fi/URN:ISBN:978-952-60-5402-5

A! Aalto-yliopisto

Tiivistelmä

Aalto-yliopisto, PL 11000, 00076 Aalto www.aalto.fi

Tekijä
Iina Vaajamo

Väitöskirjan nimi
Termodynaamisen lyijyseostietokannan kehittäminen

Julkaisija Kemian tekniikan korkeakoulu

Yksikkö Materiaalitekniikan laitos

Sarja Aalto University publication series DOCTORAL DISSERTATIONS 173/2013

Tutkimusala Metallurgia

Käsikirjoituksen pvm 09.08.2013 **Väitöspäivä** 15.11.2013

Julkaisuluvan myöntämispäivä 08.10.2013 **Kieli** Englanti

☐ **Monografia** ☒ **Yhdistelmäväitöskirja (yhteenveto-osa + erillisartikkelit)**

Tiivistelmä

Kehittyneet termodynaamiset tietokannat ja laskentaohjelmistot yhdessä CALPHAD-metodin kanssa mahdollistavat erilaisten ilmiöiden, kuten faasimuutosten ja kemiallisten reaktioiden, tarkastelun matemaattisesti termodynaamisen laskennan avulla. Tällaiset laskennat vaativat yhtenäisiä ja luotettavia termodynaamisia tietokantoja, kuten MTOX (metalli-sulfidi-oksidi-fluoridi) tietokanta, joka sisältää termodynaamisia ainearvoja systeemeistä, jotka liittyvät metallien valmistusprosesseihin. Näissä prosesseissa lyijyä pidetään usein epäpuhtautena, joka tulee prosessiin primäärisistä ja sekundäärisistä raaka-aineista. Lyijyn ja sen metalliseosten termodynamiikan syvällisempi tuntemus edesauttaa sulatus-, raffinointi- ja kuonanpuhdistusprosessien kehittämistä, joissa lyijy usein esiintyy komponenttina.

Tässä väitöskirjassa tutkittiin sulan lyijyn ja kiinteän metallifolion (Ni, Fe, Cu, Fe-Ni) keskinäistä liukoisuutta isotermisellä tasapainotustekniikalla. Kokeet toteutettiin kvartsiampullissa korkeissa lämpötiloissa. Näytteiden kemialliset koostumukset analysoitiin ICP-spektrometrillä ja EPMA:lla.

Systeemeistä tehtiin kirjallisuustutkimukset tavoitteena etsiä kaikki julkaistu kokeellinen tieto aina 1900-luvun alusta tähän päivään asti. Kirjallisuudesta löytynyt kokeellinen tieto analysoitiin kriittisesti ja valittu kokeellinen tieto käytettiin yhdessä omista kokeista saatujen tulosten kanssa systeemien liuosfaasien termodynaamisten parametriarvojen optimoimiseen CALPHAD-menetelmällä. Liuosfaasien kuvaamiseen käytettiin yksinkertaista korvausliuosmallia. Puhtaiden alkuaineiden ominaisuuksille käytettiin SGTE:n Unary-tietokantaa. Systeemit sovitettiin käyttäen MTDATA-laskentaohjelmistoa ja pienimmän neliösumman menetelmää.

Tässä työssä saatu kokeellinen tieto mahdollisti systeemien tarkempien termodynaamisten kuvausten määrittämisen. Erityisesti lyijyn liukoisuutta kiinteään metalliin monotektistä matalemmissa lämpötiloissa ei ole mitattu näin suurella tarkkuudella aikaisemmin. Kyseisten metallien liukoisuudet sulaan metalliin ovat suhteellisen hyvin tunnettuja ja tässä työssä saadut tulokset ovat yhdenmukaisia kirjallisuudessa ilmoitettujen tulosten kanssa.

Systeemien Ni-Pb, Fe-Pb, Cu-Pb ja Fe-Ni-Pb termodynaamisia kuvauksia on parannettu/luotu. Yhdenmukaisuus laskettujen faasitasapainojen ja kriittisesti valittujen kokeellisten pisteiden välillä on hyvä. Työssä saatuja sovituksia voidaan käyttää yhdessä MTOX-tietokannan kanssa laskettaessa monikomponenttisysteemien termodynaamisia ominaisuuksia ja faasitasapainoja, sekä ratkaista materiaalitekniikkaan ja metallurgiaan liittyviä ongelmia.

Avainsanat Termodynamiikka, CALPHAD, Tasapainotuskoe, Liukoisuus, MTOX, Tietokanta, Lyijy

ISBN (painettu) 978-952-60-5401-8 **ISBN (pdf)** 978-952-60-5402-5

ISSN-L 1799-4934 **ISSN (painettu)** 1799-4934 **ISSN (pdf)** 1799-4942

Julkaisupaikka Helsinki **Painopaikka** Helsinki **Vuosi** 2013

Sivumäärä 110 **urn** http://urn.fi/URN:ISBN:978-952-60-5402-5

Preface

This doctoral thesis was carried out at the Aalto University School of Chemical Technology research group of Metallurgical Thermodynamics and Modelling (TDM) during the years 2009 – 2013. First of all, I would like to express my deepest appreciation to my Professor Pekka Taskinen. You always had time to guide me when I was lost and encourage me when I felt desperate in the world of thermodynamics. I feel privileged in having you as my supervisor. Secondly, I would like to express my sincere gratitude to Dr. John Gisby for being my co-author, helping me with the MTDATA, proofreading and comments concerning my work. I owe my gratitude to Hannu Johto M.Sc. (Tech) for being my co-author, for the proofreading of this compendium but especially for being my colleague and roommate during these years. I would also like to acknowledge Professor (Emeritus) Heikki Jalkanen and Hannu Sippola Lic.Sc. (Tech) for kindly proofreading this compendium.

The thesis has been conducted with the support of Improved Sulfide Smelting (ISS) – a project of the Fimecc-ELEMET programme and Tekes – the Finnish Funding Agency for Technology and Innovation. The ISS project was supported by the following industrial sponsors: Boliden Harjavalta, Boliden Kokkola, Norilsk Nickel Harjavalta Oy and Outotec (Finland) Oy. The Jenny and Antti Wihuri Foundation, Walter Ahlström Foundation, Magnus Ehrnrooth Foundation, Finnish Cultural Foundation, Tekniikan edistämissäätiö and KAUTE Foundation have also funded the author. All the financiers are greatly appreciated.

The ISS steering group, especially Dr. Rauno Luoma D.Sc. (Tech) is acknowledged for their interest towards my work.

The research assistants of the TDM group, Kimmo Lavanti, Jani Jansson, Niko Hellstén and Markus Aspiala above all are thanked for their invaluable assistance with the experiments. Thank you also “Paja” for the help in building experimental setups.

I am grateful to the industrial sponsors for giving me the opportunity to use their analytical services. Lassi Pakkanen from the Geological Survey of Finland (GTK) is acknowledged for the EPMA analyses.

My TDM, MTG and MVT group workmates are acknowledged for their help, support and pleasant work atmosphere. I am happy to have Lotta Rintala as my “VTR buddy.” Thank you for the extremely motivating discussions and experiencing with me what it is to grow as a scientist. There are no mistakes, only lessons to be learned.

Finally I would like to thank my families, the Kainulainen and Vaajamo families, for their encouragement and just being there for me.

Matti, you are both: my co-sailor and my anchor. Thank you for all the love, patience and endless support that you have given me.

02.08.2013, Espoo

Iina Vaajamo

List of Publications

The thesis consists of a compendium and the following publications, which are referred to in the text by their Roman numerals.

I **I. Kainulainen**, P. Taskinen, J. Gisby, "A thermodynamic assessment of the nickel-lead system," CALPHAD 34 (2010) 4, 441-445.

II **I. Vaajamo**, P. Taskinen, "A thermodynamic assessment of the iron-lead binary system," Thermochimica Acta 524 (2011) 56-61.

III **Iina Vaajamo**, Hannu Johto, Pekka Taskinen, "Solubility study of the copper-lead system," International Journal of Materials Research 104 (2013) 4, 372-376.

IV **I. Vaajamo**, P. Taskinen, J.A. Gisby, "A solubility study and thermodynamic description of the system Fe-Ni-Pb," CALPHAD 42 (2013) 66-75.

V **I. Vaajamo**, P. Taskinen, J.A. Gisby, "An extensive slag database: Lead-ing the way." In: Proceedings of the Copper 2013 International Conference, 2013, December 1-4, Santiago, Chile. Accepted for publication.

Author's contribution

Publication I: "A thermodynamic assessment of the nickel-lead system"

A literature survey was done by the author. A thermodynamic pre-assessment was done in collaboration with Dr. John Gisby. The assessment was finalized by the author with some additional experimental data from the literature. The author wrote the first version of the manuscript and edited the final version based on the input from the co-authors.

Publication II: "A thermodynamic assessment of the iron-lead binary system"

A literature survey and the thermodynamic assessment were done by the author. The author planned the equilibration experiments and executed them together with her research assistant. The EPMA analyses were conducted at the Geological Survey of Finland (GTK). The ICP analyses were conducted at Norilsk Nickel Harjavalta Oy. The author analysed the results, wrote the first version of the manuscript and edited the final version based on the input from the co-author.

Publication III: "Solubility study of the copper-lead system"

A literature survey of the solid solubilities of copper and lead was done by the author. The Cu-Pb thermodynamic assessment was done by Hannu Johto M.Sc. (Tech.). The author planned the equilibration experiments and executed them. The EPMA analyses were conducted at the Geological Survey of Finland (GTK). The ICP analyses were conducted at Boliden Harjavalta. The author analysed the results, wrote the first version of the manuscript and edited the final version based on the input from the co-authors.

Publication IV: "A solubility study and thermodynamic description of the system Fe-Ni-Pb"

A literature survey and the thermodynamic assessments of the systems Ni-Pb and Fe-Ni-Pb were done by the author. The author planned the equilibration experiments and executed them together with her research assistant. The EPMA analyses were conducted at the Geological Survey of Finland (GTK). The Ni-Pb ICP analyses were conducted at Norilsk Nickel Harjavalta Oy and the Fe-Ni-Pb analyses at Outotec (Finland) Oy Pori Research Center. The author analysed the results, wrote the first version of the manuscript and edited the final version based on the input from the co-authors.

Publication V: "An extensive slag database: Lead-ing the way"

The author wrote the first version of the manuscript, excluding the Chapter "MTOX database," and edited the final version based on the input from the co-authors. The author calculated the electric furnace slag cleaning case example with the help of Professor Pekka Taskinen. Dr. John Gisby calculated the viscosity and electrical conductivity examples.

List of Symbols and Abbreviations

Symbols

A_n	Margules parameter
a	activity
a-g	coefficients of heat capacity function
A-G	coefficients of Gibbs energy temperature dependence function
c_P	molar heat capacity, constant pressure
C_i	the calculated value of property i
D	diffusion coefficient
E_i	the experimental value of property i
G	Gibbs energy
$^{\circ}G$	standard Gibbs energy
g	structure dependent function of temperature
H	enthalpy
i	property
$i,j,k...N$	components
k	coverage factor
L	interaction parameter
n	number of moles
n	the number of properties (data items) to be reproduced
P	pressure
p	structure dependent empirical constant
R	gas constant
S	entropy
S	weighted sum of squares of errors
T	temperature
T^*	critical temperature
T_C	Curie temperature
T_N	Néel temperature
u	uncertainty factor
$U_{(}t_{v)}$	expanded uncertainty
$u_{(}t_{v)}$	standard error
U_i	uncertainty associated with the values E
V	volume
v	geometric composition term
W_i	weight assigned to a property i
x	mole fraction
Z	thermodynamic property

Superscripts

$^{\circ}$	standard state
^{E}	excess
$^{n...m}$	order of polynomial
^{id}	ideal
^{magn}	magnetic
^{pres}	pressure
$^{\theta}$	phase

Subscripts

$_{i,j,k}$	components

Greek letters

α_n, β_n	parameters for activity coefficient clause
$\beta_{\circ}$	average magnetic moment
γ	activity coefficient
$\theta...\varphi$	phase
μ	chemical potential
τ	$\tau=T/T^*$ where T^* is the critical temperature

Abbreviations

BCC_A2	Body-centred cubic, with the Strukturbericht symbol
BOHA	Boliden Harjavalta, Finland
CALPHAD	CALculation of PHAse Diagrams
DIN IEC 751	Resistance thermometer standard
DMM	Digital Multimeter
EDS	Energy Dispersive Spectrometer
EMF	Electromotive force
EPMA	Electron Probe Microanalysis
FCC_A1	Face-centred cubic, with the Strukturbericht symbol
GTK	Geological Survey of Finland
ICP	Inductively Coupled Plasma
MIRO	Mineral Industry Research Organization, UK
MTDATA	Thermochemical software from NPL
MTOX	Metal-oxide-sulphide-fluoride thermodynamic database
NNH	Norilsk Nickel Harjavalta Oy, Finland
NPL	National Physical Laboratory, UK
ORC	Outotec (Finland) Oy, Pori Research Center, Finland
SEM	Scanning Electron Microscope
SER	Stable Element Reference
SGTE	Scientific Group Thermodata Europe

WDS	Wavelength Dispersive Spectrometer
WEEE	Waste Electrical and Electronic Equipment

Table of Contents

1. Introduction

1.1 Background

Lead is considered as an impurity in many metal-making processes. It may come to the process from the primary raw materials, i.e. natural minerals, or from secondary raw materials such as WEEE (Waste Electrical and Electronic Equipment) [1,2]. The demand for metals is continuously increasing while raw materials are progressively being depleted and becoming more challenging to process [3,4]. Secondary raw materials can contain components that do not exist in the primary ore-bearing raw materials and that behave quite differently when processed [5]. In the smelting step, the metal-slag and metal-matte equilibria are of significant importance as to environmental sustainability and valuable metal recoveries [5]. Better understanding of the thermodynamic behaviour and phase equilibria of lead could help in developing smelting and refining properties including slag-cleaning operations, where lead is often reduced back to the crude metal. The phenomena that take place during these processes are complex, as yet impossible to investigate *in situ* and sometimes even impossible to investigate experimentally.

The availability of advanced thermodynamic databases and software and the CALPHAD (CALculation of PHAse Diagrams) method [6-8] allow smelting, refining and slag cleaning phenomena to be evaluated mathematically by thermodynamic calculations. Thermodynamic calculations require internally consistent and reliable thermodynamic databases with reasonable coverage. At present, building these databases is one major task being undertaken by the CALPHAD community.

The National Physical Laboratory's (NPL) MTOX (metal-oxide-sulphide-fluoride) thermodynamic database [9,10] covers equilibria data for the metallic, oxide, sulphide and fluoride systems related to metal smelting and refining processes. The MTOX database has been created under the guidance of the Mineral Industry Research Organization (MIRO) and is mainly funded by industrial partners. The current coverage of the MTOX database is presented in [V] but the development work is continuous,

mainly executed by NPL, but also including contributions from the academic partners.

1.2 Objective of the thesis

The objectives of this thesis were:

1. to gain new experimental solubility data concerning lead alloys Ni-Pb, Fe-Pb, Cu-Pb and Fe-Ni-Pb, and
2. to use these data together with literature data to derive the thermodynamic model parameters of the aforementioned lead alloy systems to be consistent with the MTOX database.

Although some of the lead alloy systems covered in this thesis have been of interest to many scientists, experimental data are still somewhat scarce. At an early stage of research, it was noticed that the lead solubility in solid metal was not known experimentally in any of these systems, apart from one rather inaccurate point of the Cu-Pb system. An equilibration technique was chosen to discover the mutual solubilities of the components. This is the most traditional and most widely used method for phase diagram determination [11]. As the liquidus temperatures at the lead-rich ends of these systems are fairly well known, the obtained data could be used for validation of the experimental data reported earlier in the literature.

The obtained new solubility data together with critically selected literature data were used to optimize the thermodynamic interaction parameters using MTDATA software [12].

1.3 New scientific information

The new scientific information obtained within this thesis consists of the experimentally measured mutual solubilities of the Ni-Pb, Fe-Pb, Cu-Pb and Fe-Ni-Pb systems and the new improved thermodynamic descriptions of them. Two experimental set-ups were built and reported: a chamber furnace and a horizontal tube furnace. The lead solid solubility in nickel, iron, copper and iron-nickel has not been experimentally determined previously in the literature with adequate accuracy, at least to the best knowledge of the author. The solubilities of nickel, iron, copper and iron-nickel in molten lead have been reported previously in the literature and the measured solubilities obtained within this work were compared with the data from the literature. Experimental literature data were found that have not been used in the previously reported Ni-Pb and Cu-Pb binary systems assessments. Using these new experimental data enabled us to obtain more accurate thermodynamic descriptions of the Ni-Pb, Fe-Pb and Cu-Pb binary systems than those reported earlier. The thermodynamic

assessment of the Fe-Ni-Pb system has not been reported in the literature before.

1.4 Applications

As the nature of this kind of research is basic research, the lead alloy database together with the MTOX database has great potential for practical applications.

Thermodynamic calculations can be used in designing industrial processes, e.g. to obtain optimal process parameters and thus optimize the best possible recovery of precious metals and treatment of impurities. [10,13-15]. These data can be used in developing automation of processes such as steelmaking, and to understand and solve problems related to chemical reactions involving complex combinations of many components and phases [16].

Knowledge of the solubility of lead in some metal alloys can prevent the "intermediate temperature embrittlement" caused by the low solubility of lead in these metal alloys, thus affecting the tensile properties of the alloys [17].

The use of thermodynamic software together with a suitable thermodynamic database means that fewer experiments are needed, hence saving time and money.

Additionally, better knowledge of the thermodynamic behaviour of lead alloys could be applied in the development of lead-free solder alloys [18], bearing metals [19], Generation IV nuclear power plants [20], recycling of metals [5,21] and of lead acid batteries [22], and impurity removal from steel scrap [23].

1.5 Structure of the thesis

This thesis consists of four scientific peer-reviewed journal publications [I-IV], one peer-reviewed conference publication [V] and the present compendium. The publications have been either published or accepted for publication and are attached in the Appendices.

Chapter 2 of the thesis presents the CALPHAD method and gives an insight into the state-of-the-art and the benefits of the method. Chapter 3 covers the thermodynamic models for pure and solution phases used in this work. The viscosity and electrical conductivity models for liquid oxides covered in [V] are left outside of the scope of this thesis. Chapter 4 presents the actual assessment procedure. Chapter 5 contains a detailed description of the experiments that has been reported in [II-IV] and in [24-26]. The results and discussion are given in Chapter 6, concluding with the conclusions in Chapter 7.

2. CALPHAD method

The acronym CALPHAD comes from the words CALculation of PHAse Diagrams. It is a method of deriving the thermodynamic functions of a system using critically evaluated and selected experimental data. Phase diagrams are graphical presentations of the values of thermodynamic variables, often temperature and composition, at equilibrium state among the phases in the system [27].

The development work of the CALPHAD method is the result of the work of many scientists [7,28]. In the 1970s, Kaufman and Bernstein [6] introduced the first general description of the CALPHAD method [7,8]. Since then, the method has been developed alongside the development of computers. Nowadays, it is used widely in developing larger thermodynamic databases and as a tool in solving problems related to materials science, materials engineering and in thermochemistry [8,13,29-31].

In CALPHAD method type calculations, Gibbs energy, *G,* is used to determine the thermodynamic properties of each phase of the system. The description is semi-empirical, resting on the thermodynamic models developed for Gibbs energy and critically evaluated and selected experimental data. The models describe the Gibbs energy of each phase in a system within a chosen temperature and composition range. The total Gibbs energy of a system is minimized by adjusting the model parameters so that the best possible agreement between the measured and calculated data is obtained. The optimized parameters are stored on a thermodynamic database. The data can be estimated from the lower-order systems to higher-order systems.

All the thermodynamic properties and the phase diagrams can be represented and stored by means of a small set of coefficients [27]. Once a multicomponent database is created, it enables a visual and numerical examination of the thermodynamic properties of a specific system. In practice, it means that with special thermodynamic software, such as MTDATA [12], ThermoCalc [32] and Factsage [33], it is possible to calculate properties and simulate the transformations of multicomponent

systems using the modelled Gibbs energy and its derivatives, such as enthalpy, entropy, specific heat, chemical potential, molar volume, volume expansion, isothermal compressibility and bulk modulus [8]. Besides calculating phase diagrams and thermodynamic properties of a system, it can be used to calculate metastable states, and simulate diffusion, solidification and evolution of microstructures [8,14,29]. Multicomponent databases are also used in calculating viscosities and electrical conductivities [V].

Today, “CALPHAD development work” is to a large degree focused on building multicomponent databases. It has been agreed to use the SGTE (Scientific Group Thermodata Europe) Unary database for pure elements, reported originally by Dinsdale [34]. Quite often databases concentrate on a certain material group, to give a few examples besides MTOX [9,10]: platinum-based superalloys [35,36], lead-free solder alloys [18], steelmaking [16] and a zirconium alloy database for nuclear energy purposes [37].

In order to obtain a good thermodynamic description of a higher-order system, the lower-order (unary, binary and ternary) systems need to be accurate. Experience to date has shown that reliable binary assessments are of major importance, even in the case of a ternary system, being more important than the ternary terms [11]. For this reason, it is very important to have accurate thermodynamic descriptions of the unary and binary systems.

3. Thermodynamic models

Gibbs energy, *G,* is chosen as the modelled thermodynamic function, as many of the experimental data have been measured and most technical processes work at a known pressure and temperature. At constant temperature, pressure and composition, a closed system will approach an equilibrium state, which minimizes the Gibbs energy [27]. Gibbs energy also has a special role in thermodynamics, because it is possible to derive other thermodynamic functions from it [8], as mentioned in Chapter 2. Thus, Gibbs energy is an unambiguous state variable for describing a system. The Gibbs energy of a system can be expressed in terms of enthalpy, *H*, temperature, *T,* and entropy, *S*.

$$G = H - TS \tag{1}$$

Thermodynamic software are based on the minimization of the total or integral Gibbs energy of a multicomponent system as a function of temperature, pressure and composition. The integral Gibbs energy is calculated as a sum of all the Gibbs energies of the phases taking part in the equilibrium [8,38]. At constant temperature and pressure, the integral Gibbs energy is expressed as

$$G = \sum_{\theta}^{\varphi}\left(\sum_{i}^{N} x_i^{\theta} G_i^{\theta}\right) \tag{2}$$

where $x_i\theta$ is the mole fraction of component i of the phase θ and G^{θ}_i is the Gibbs energy of a component i of the phase θ. Alternatively, the integral Gibbs energy can be expressed in terms of the chemical potential, μ_i, i.e. the partial molar Gibbs energy of the system components $i...N$ in isobaric and isothermic systems. The relation of the mole fraction, x_i, to the amount of component i, n_i, is $x_i = n_i / \sum n_i$.

$$G = \sum_{i}^{N} x_i G_i = \sum_{i}^{N} x_i \mu_i \qquad (3)$$

The Gibbs energies of different phases are modelled separately and described with thermodynamic models. The models are divided into mathematical and physical models, of which mathematical models are analytical descriptions of the excess Gibbs energy of the system as a function of temperature, pressure and composition. They do not describe any physical property [39] as the physical models do. Thermodynamic models have been discussed in many publications, for instance [7,8,27,40].

The general form of the Gibbs energy, G^{θ}, of a solution phase θ for the whole composition range is often expressed as a sum of different Gibbs energy contributions, as shown in a general form in Equation (4):

$$G^{\theta} = {}^{\circ}G^{\theta} + {}^{id}G^{\theta} + {}^{E}G^{\theta} + {}^{magn}G^{\theta} + {}^{pres}G^{\theta} + \ldots \qquad (4)$$

where the first two terms define the ideal solution, ${}^{id}G^{\theta}$, with respect to its standard state, ${}^{\circ}G^{\theta}$, and then treat the non-ideal part with the excess Gibbs energy, ${}^{E}G^{\theta}$. The mathematical form of these terms depends on the solution model used. The last two terms in Equation (4) are the magnetic, ${}^{magn}G^{\theta}$, and pressure dependencies, ${}^{pres}G^{\theta}$, for the Gibbs energy, respectively. The pressure dependency of the Gibbs energy is expressed with Murnaghan's model [41] but it is normally ignored due to isobaric conditions.

The analytical form of the different Gibbs energy contributions to the simple substitutional model that were used in the present thesis is presented below.

3.1 Pure elements

The Gibbs energy of a pure element depends on two independent variables, i.e. temperature and pressure, P. In relation to Equation (1), the G, H and S are functions of temperature at constant pressure through heat capacity, c_P. At constant pressure, enthalpy and heat capacity have the following differential relationship:

$$c_P = \left(\frac{\partial H}{\partial T} \right)_P \qquad (5)$$

The change of enthalpy, ΔH, as a function of temperature can be obtained by integrating c_P relative to a reference state of 298.15 K (SER, see below):

$$\Delta H = H(T) - H(298.15) = \int_{298.15}^{T} c_P dT \quad (6)$$

For entropy, the similar isobaric relation with heat capacity is written as

$$\frac{c_P}{T} = \left(\frac{\partial S}{\partial T}\right)_P \quad (7)$$

Integration c_P/T over a temperature interval from 298.15 K to T gives

$$\Delta S = S(T) - S(298.15) = \int_{298.15}^{T} \frac{c_P}{T} dT \quad (8)$$

Like enthalpy and entropy functions, heat capacity function is a non-continuous function of temperature. For liquids it is usually constant but for crystalline phases the temperature dependency of the Gibbs energy often changes, especially in the vicinity of transition points [42]. Experience has shown that heat capacity can be presented mathematically for pure substances and homogenous phases with sufficient accuracy based on an empirical equation by Kelley [43] in quite wide temperature ranges [42]:

$$c_P = a + bT + cT^2 + dT^3 + e/T^2 + f/T^3 + \sum g_n T^n \quad (9)$$

where the coefficients $a...g$ of the polynomial are fitted to experimental data. The equation is valid for a temperature range with no phase transformations. Heat capacity values are normally presented in thermochemical data books, e.g. in Barin [42].

Equation (9) can be included in Equation (1) using the enthalpy and entropy relations in Equations (6) and (8), which gives

$$G(T) = H(298.15) + \int_{298.15}^{T} c_P dT - T\left(S(298.15) + \int_{298.15}^{T} \frac{c_P}{T} dT\right) \quad (10)$$

This gives the following expression for the Gibbs energy temperature dependence, where coefficients A and B contain contributions from both $\Delta H(298.15)$ and c_P, and $\Delta S(298.15)$ and c_P, respectively. The latter terms are related to the coefficient of the standard c_p equation. [38]

$$G(T) = A + BT + CTlnT + DT^2 + ET^3 + F/T + \sum G_n T^n \quad (11)$$

Thermodynamic variables, such as *G* and *H,* cannot be given as absolute values but differences between two well-defined states. That is why they are tied to a reference state. The reference state should always be the same inside a thermodynamic database, otherwise the properties are not compatible. The reference state for enthalpy adopted currently, and within SGTE, is that the enthalpy of an element in its stable form at 298.15 K and 1 bar pressure is defined to be zero, denoted by the superscript SER (Stable Element Reference).

$$H_i^{SER}\ (298.15\ K, 1\ bar) = 0 \quad (12)$$

This means that Equation (11) of the Gibbs energy of a pure element (or a stoichiometric component *i* of a phase θ) is commonly written as

$$^{o}G_i^{\theta}(T) - H_i^{SER}(298.15) = A + BT + CTlnT + DT^2 + ET^3 + F/T + \sum G_n T^n \quad (13)$$

where *A*...*F* are a standard set of six coefficients obtained by assessing and fitting the measured thermodynamic properties of the element and component in question, and are stored on a thermodynamic database. Further coefficients G_n are sometimes added if required. The difference in Gibbs energy between a phase and a stable reference phase with the same elemental composition (lattice stability) can be typically measured and thus calculated by subtracting one set of assessed coefficients from another. The coefficients for pure elements, (in Equation (13) the coefficients *A*-*G*), known as unary data, have been derived by SGTE and were reported originally by Dinsdale [34].

The reference state for entropy is obtained from the third law of thermodynamics, which states that the entropy of a chemically homogenous crystalline material is zero at the absolute zero temperature. This principle allows calculation of the absolute values of entropy of pure substances solely from heat capacity. [42] For practical reasons, the entropy value is often reported against *S*(298.15) instead of zero Kelvin.

3.2 Ideal solutions

Solution phases differ from the stoichiometric (unary) phases in that they have a variable composition. The concentration dependence of the Gibbs energy is taken into account through chemical potential, μ. Chemical potential is a measure of the change of Gibbs energy due to the addition of

component *i* to the system, and is thus expressed as μ_i. For a homogenous system, it is described as

$$\mu_i = G_i = \left(\frac{\partial G}{\partial n_i} \right)_{T,P,n_{j \neq i}} \quad (14)$$

where *G* is the Gibbs energy of a solution, n_i is the number of moles of component *i*. This is related to Equation (3) and when differentiated it gives

$$dG = \sum_i^N n_i d\mu_i + \sum_i^N \mu_i dn_i \quad (15)$$

When combining this with the derivative *dG* of Equation (1), the following relation of the Gibbs energy temperature, pressure and composition dependency is obtained:

$$dG = -SdT + VdP + \sum_i^N \mu_i dn_i \quad (16)$$

where *V* denotes volume.

In equilibrium and at constant temperature and pressure, Equation (16) is reduced to Equation (17). This is called the Gibbs-Duhem equation:

$$\sum_i^N \mu_i dn_i = 0 \quad (17)$$

Chemical potential can be presented as in Equation (18) in terms of activity, *a*, which describes the characteristic features of a solution relative to its standard state, ${}^o\mu_i$, as a function of pressure, temperature and composition:

$$RT \ln a_i = \mu_i - {}^o\mu_i \quad (18)$$

From the above, it can be seen that the value of activity is dependent on the standard state value. Without reporting the standard value, chemical potentials or activities cannot be described unambiguously.

For ideal (substitutional) solutions the activity of the component *i* is equal to its mole fraction:

$${}^{id}a_i = x_i \quad (19)$$

Thus, Equations (2-4, 18, 19) can be expressed as

$$G^{\theta} = {}^{o}G^{\theta} + {}^{id}G^{\theta} = \sum_{i}^{N} x_i^{\theta} \cdot {}^{o}G_i^{\theta} + RT \sum_{i}^{N} x_i^{\theta} \ln x_i^{\theta} \tag{20}$$

3.3 Non-ideal solutions

Even before automatic computation became common, the non-ideality or the 'excess Gibbs energy' of a solution was described with suitable equations presenting the activity coefficients [44]. The activity coefficient, γ_i of a component *i,* is the ratio of its activity, a_i, and mole fraction, x_i:

$$\gamma_i = \frac{a_i}{x_i} \tag{21}$$

This gives the following expression to the different Gibbs energy expressions:

$$G^{\theta} = {}^{o}G^{\theta} + {}^{id}G^{\theta} + {}^{E}G^{\theta} = \sum_{i}^{N} x_i^{\theta} \cdot {}^{o}G_i^{\theta} + RT \sum_{i}^{N} x_i^{\theta} \ln x_i^{\theta} + RT \sum_{i}^{N} x_i^{\theta} \ln \gamma_i^{\theta} \tag{22}$$

The excess properties of the mixing of the solution phases have been described by empirical equations as a power series [45]. Among the first were Margules-type [46] equations [45,47,48], where (any) excess property, ${}^{E}Z$, is presented with respect to the mole fraction as

$${}^{E}Z = x_i x_j \sum_{n}^{m} A_n x_j^n = x_i x_j (A_0 + A_1 x_j + A_2 x_j^2 + \ldots + A_m x_j^m) \tag{23}$$

The Margules parameters for excess Gibbs energy, A_k, are calculated from the experimental activity coefficient as a power series of composition. If they are zero, it is an ideal solution [48].

$$\ln \gamma_i = \sum_{n}^{m} \alpha_n x_j^{\,n} = \alpha_0 + \alpha_1 x_i + \alpha_2 x_i^2 + \ldots + \alpha_m x_i^m \tag{24}$$

$$\ln \gamma_j = \sum_{n}^{m} \beta_n x_j^{\,n} = \beta_0 + \beta_1 x_i + \beta_2 x_i^2 + \ldots + \beta_m x_i^m$$

According to the Gibbs-Duhem Equation (17), the first two terms are identically zero if the solution model is valid from $x_i \in (0,1)$, i.e.

$$a_o = b_o = 0 \text{ and } a_1 = b_1 = 0 \qquad (25)$$

Eq. (23) is often modified to take into account the composition dependency between species. This was suggested by Redlich and Kister [44] and is presented in Equation (26) in a general form for a binary system *i,j*. It considers the complete mixing of the species on the same sublattice, i.e. the component of a crystalline phase has the same probability of occupying any site in the unit cell or lattice [8].

$$^{E}G^{\theta} = x_i^{\theta} x_j^{\theta} \sum_{n}^{m} {}^{n}L_{ij} (x_i^{\theta} - x_j^{\theta})^n \qquad (26)$$

where ${}^{n}L_{ij}$ is the temperature-dependent binary interaction parameters, to be estimated based upon experimental data. In the current work, each parameter is a linear function of temperature, for example ${}^{n}L_{ij} = {}^{n}L^{o}_{ij} + {}^{n}L^{1}_{ij} T$. m is the order of the polynomial for each binary system. x_i and x_j are the mole fractions of the components in the phase. Because of thermodynamic consistency and Equations (5) – (13), the mathematical form of the temperature dependence of the interaction parameters is the same as that of the Gibbs energy.

As the experimental data on ternary and in particular higher-order systems is very limited, the calculation of equilibria of multicomponent alloys are strongly based on the constituent binary alloys [49]. Various methods exist for interpolating the properties of a ternary system based on the binary systems [49-52]. The most common models are the geometric models by Kohler [53], Kohler/Toop [54], Muggianu [55] and Muggianu/Toop [50]. [52] They are based on geometric reasoning of how to add together the binary systems contributions.

MTDATA uses the Muggianu method [55], which treats the contributions of the three binary systems in the same way. The excess Gibbs energy of the ternary solution is estimated at a certain composition point from the excess Gibbs energies in three binary systems at points 1, 2, 3 (Figure 1). Experimental ternary data can be included in the optimization for estimating empirical ternary interaction terms [51,56]

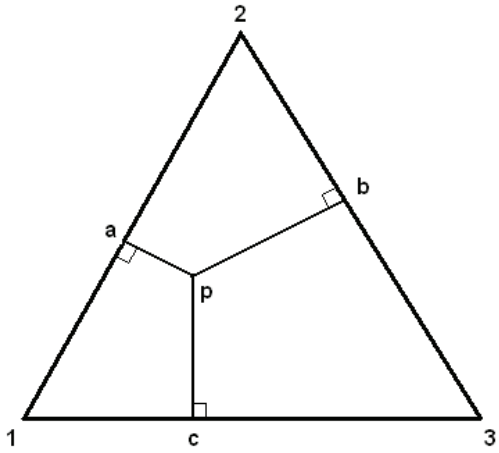

Figure 1. Geometric model from Muggianu for estimating ternary thermodynamic properties from assessed binary data 1-2, 2-3, 1-3. The triangle is modified from Muggianu [55].

Thus, for a ternary system, the Redlich-Kister polynomial is written as in Equation (27):

$$
\begin{aligned}
{}^{E}G^{\theta} = {} & x_i^{\theta} x_j^{\theta} \sum_{n}^{m} {}^{n}L_{ij}(x_i^{\theta} - x_j^{\theta})^n + x_i^{\theta} x_k^{\theta} \sum_{n}^{m} {}^{n}L_{ik}(x_i^{\theta} - x_k^{\theta})^n + \\
& x_j^{\theta} x_k^{\theta} \sum_{n}^{m} {}^{n}L_{jk}(x_j^{\theta} - x_k^{\theta})^n + x_i^{\theta} x_j^{\theta} x_k^{\theta} (v_i \, {}^{0}L_{ijk} + v_j \, {}^{1}L_{ijk} + v_k \, {}^{2}L_{ijk})
\end{aligned}
\tag{27}
$$

where L_{ijk} are the temperature-dependent ternary interaction parameters to be estimated based upon experimental data. x_i^{θ}, x_j^{θ}, x_k^{θ} are the mole fractions of the component in phase θ. According to [51], when using the Muggianu model [55], the v_i, v_j, v_k in Equation (27) are expressed as

$$v_i = x_i^{\theta} + (1 - x_i^{\theta} - x_j^{\theta} - x_k^{\theta})/3 \tag{28a}$$

$$v_j = x_j^{\theta} + (1 - x_i^{\theta} - x_j^{\theta} - x_k^{\theta})/3 \tag{28b}$$

$$v_k = x_k^{\theta} + (1 - x_i^{\theta} - x_j^{\theta} - x_k^{\theta})/3 \tag{28c}$$

As a result of the equations above, the following Equation (29) for the Gibbs energy of a phase θ without magnetic contributions is obtained for the simple substitutional model that was used in the present thesis. The excess part is presented with Equation (26) for a binary system and Equation (27) for a ternary system:

$$G^{\theta} = \sum_{i}^{N} x_i^{\theta} \cdot {}^{o}G_i^{\theta} + RT \sum_{i}^{N} x_i^{\theta} \ln(x_i^{\theta}) + {}^{E}G^{\theta} \tag{29}$$

3.3.1 Magnetic contribution

Some physical features, such as ferromagnetic or antiferromagnetic transitions, are modelled separately by adding a magnetic contribution term ${}^{magn}G^{\theta}$ to the integral Gibbs energy, as presented in Equation (4). Ferromagnetic transitions do not depend smoothly on the composition [8]. As an example, Figure 2 shows the molar heat capacity of nickel, where the heat capacity shows a sharp peak at the ferromagnetic transition temperature of 633 K, i.e. the Curie temperature.

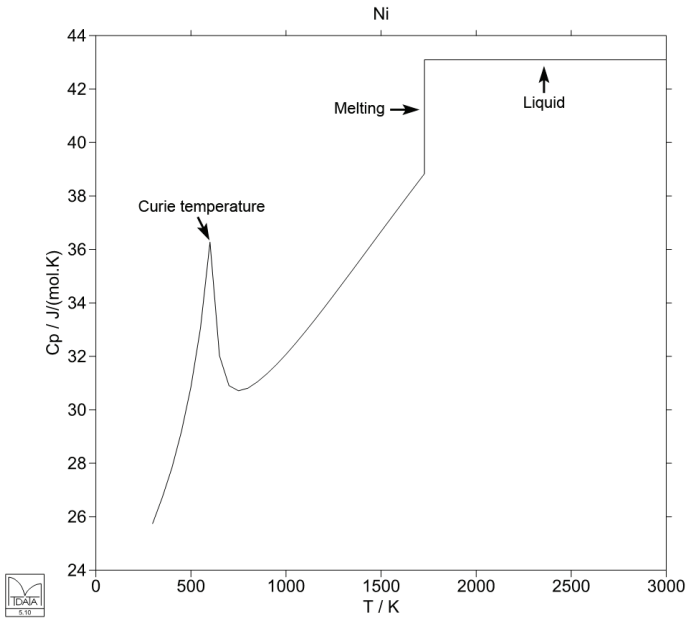

Figure 2. Molar heat capacity, c_P of nickel showing the ferromagnetic transformation, i.e. the Curie temperature.

Currently, the magnetic transformation of pure elements at the magnetic transition temperature is described using the model introduced by Inden [57] and modified by Hillert and Jarl [58]. According to them:

$${}^{magn}G^{\theta} = RTg(\tau)\cdot \ln(\beta_0^{\theta}+1) \qquad (30)$$

where β_o denotes the average magnetic moment, $\tau = T/T,^*$ where T^* is the critical temperature, either the Néel temperature, T_N, for antiferromagnetic materials or the Curie temperature, T_C, for ferromagnetic materials. β_o and T^* are modelled as a function of composition using the Redlich-Kister polynomial [44]. g is a structure-dependent function of temperature. The difference between the pure magnetic substances and solution phases is that the β_o and T^* are functions of composition [38]:

$$g(\tau)=\begin{cases}1-\frac{1}{D}\left[\frac{79\tau^{-1}}{140p}+\frac{474}{497}\left(\frac{1}{p}-1\right)\left(\frac{\tau^{3}}{6}+\frac{\tau^{9}}{135}+\frac{\tau^{15}}{600}\right)\right] \\ -\frac{1}{D}\left(\frac{\tau^{-5}}{10}+\frac{\tau^{-15}}{315}+\frac{\tau^{-25}}{1500}\right)\end{cases} \quad (31)$$

The upper equation is used when $\tau \leq 1$, and the lower when $\tau > 1$. D receives the form presented in Equation (32):

$$D=\frac{518}{1125}+\frac{11692}{15975}\left(\frac{1}{p}-1\right) \quad (32)$$

where p is an empirical constant depending on the structure [57]. For FCC_A1 p=0.28 and for BCC_A2 p=0.4.

The Inden-Hillert-Jarl magnetic model has been widely used but also lately criticized for not being able to describe the Fe-Ni system [59]. A new magnetic model has recently been proposed [60].

Figure 3 illustrates a summary of the thermodynamic models and a linkage between Chapters 2-4. When carrying out a thermodynamic assessment with the CALPHAD method, a sum of the Gibbs energies for each phase is described as a function of temperature, pressure and composition. For a given set of constraints, such as fixed pressure, temperature and composition, the Gibbs energy minimization algorithms find the amounts of the various phases and the composition of the solution phases which give a global minimum in the total Gibbs energy of the system [61]:

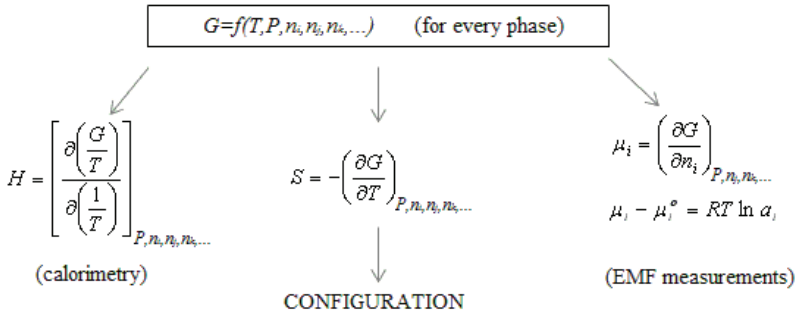

Figure 3. Summary of the Gibbs energy and other thermodynamic functions derived from it. The figure is originally from [61].

From the Gibbs energy, other thermodynamic functions, such as enthalpy, entropy and chemical potential are derived in order to determine the contributions of the pure phase components, and the ideal and non-ideal mixing of the chosen phase components. The enthalpy, entropy and chemical potential can be measured by calorimetric, electromotive force (EMF) and vapour pressure techniques and/or by calculating with ab initio methods. The ideal mixing of the phase components is related to the entropy of configuration of a phase, which treats the number of possible arrangements of the atoms in the phase. On the other hand, the Gibbs energies can be determined by means of independent phase diagram experiments at known pressure, temperature and composition, which is the great benefit of the CALPHAD method.

4. The assessment procedure

The assessment procedure means the overall task of deriving the interaction model parameters from compiled and critically evaluated experimental data. The assessment procedure flowsheet used in this work in presented in Figure 4.

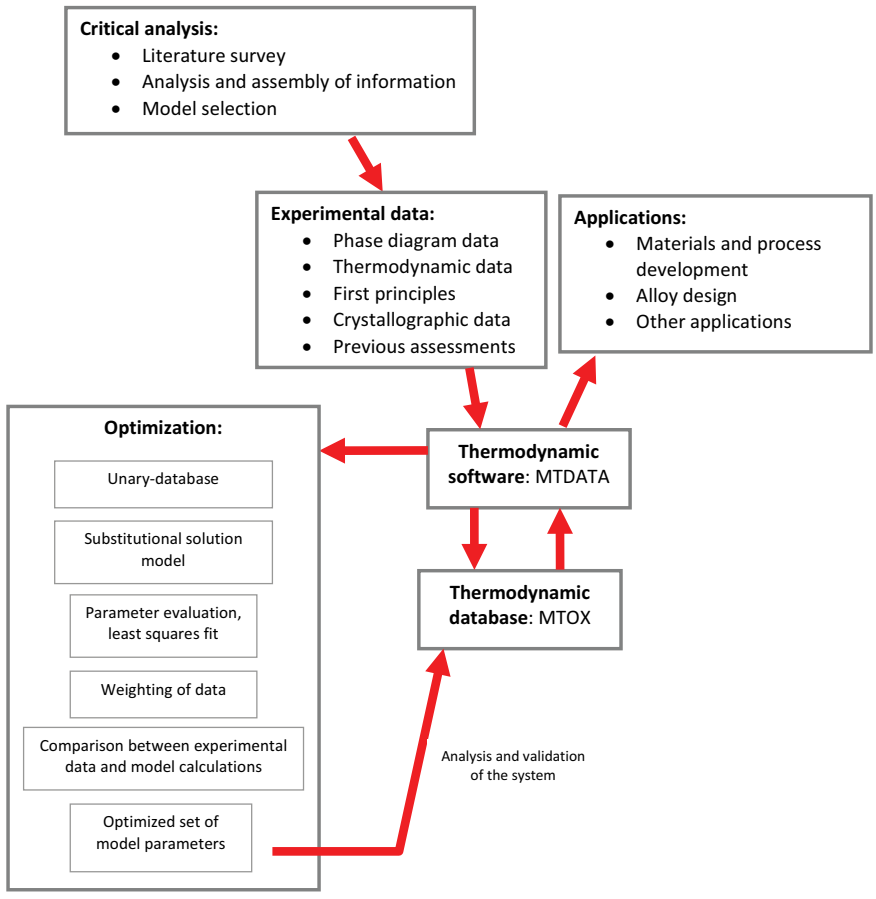

Figure 4. The assessment procedure flowsheet used in this work.

The assessment procedure starts with a thorough literature survey and compilation of the previous thermodynamic assessments, experimental phase diagram and thermodynamic data, crystallographic data and increasingly data from first principles calculations based on ab initio methods [63]. As the thermodynamic assessment is based on the experimental data used in the assessment, critical analysis of the data is essential [8,29,30,64]. The experimental data that are not used in the assessment can be used in the validation of the model. Each phase needs to be described with a thermodynamic Gibbs energy model, perhaps describing a specific physical or chemical feature. The models describe the Gibbs energy of each phase in a system, not just within the stable region but the entire temperature and composition range. When building a multicomponent database, the models for each phase need to be the same in order to be compatible in the subsequent simulations. The data for the pure elements and stoichiometric phases are taken from the unary database [34]. Another model is used for the solution phases, in this work the substitutional solution model, where the non-ideal interactions are described with the Redlich-Kister polynomial [44], see Equations (26-27). The Fe-Ni binary system [IV] was taken from the MTOX database and was not assessed by the author. The coefficients of the thermodynamic model are optimized by fitting the experimental and the calculated data during the assessment. The thermodynamic assessments were made using MTDATA software, versions 4.82, 5.03 and 5.10. The magnetic properties described with the model proposed by Inden [57] and later modified by Hillert and Jarl [58], see Equation (30), were also taken from the MTOX database and not assessed by the author.

The object function minimized during optimization runs is a weighted sum of squares of errors, S:

$$S = \sum_{i=1}^{n} W_i \left[\frac{(C_i - E_i)}{U_i} \right]^2 \qquad (33)$$

where i is the property, n is the number of properties (data items) to be reproduced, C_i is the calculated value of property i, E_i is the experimental value of property i, W_i is the weight assigned to property i, U_i is the uncertainty associated with the values E. W_i is one for all the data items included in the assessment by default but zero for the excluded observations.

During optimization, experimental data is added gradually, possibly giving it a different weighting and/or uncertainty, often resulting in many optimization rounds. The assessment process depends greatly on the assessor [64], thus making thermodynamic assessments ‘not exact science’. If possible, after optimization the model will be validated with data that was not used in the assessment. Thermodynamic coefficient values are stored on a database. The smaller databases are combined into a larger database (e.g. MTOX) and used in calculations of different applications in much larger systems. [8]

5. Equilibration experiments

In the adopted experimental technique, liquid lead was equilibrated with solid metallic foil in specially formed quartz ampoules. Samples were mixed during the experiment to accelerate diffusion and homogenization. This method made it possible to obtain two solubility limit points from the ends of the phase diagram (a tie line) in one experiment. A chamber furnace was used at first but during the experiments some development ideas led to the building of a vertical tube furnace.

Kleppa and Weil [65] used a similar kind of test method when investigating the solubility of copper in liquid lead. The experimental method has been reported in the publications [II-IV]; a more detailed description is given below.

5.1 Materials

The test materials used in the experiments were commercial metallic granules and foils and are listed below along with the purity, manufacturer and characteristic size. According to the manufacturer, the Fe-Ni foil purity was about 99 % but could not be guaranteed. For this reason, the chemical composition of the foil was analysed with a Scanning Electron Microscope Energy Dispersive Spectrometer (SEM-EDS), which established the purity to be 99.4 %.

- Lead granule, Alfa Aesar 99.999 %, 0.6-3.0 mm
- Ni foil, Alfa Aesar 99.994 %, 0.1 mm
- Fe foil, Alfa Aesar 99.99 %, 0.1 mm
- Cu foil, Alfa Aesar Puratronic® 99.999 %, 0.1 mm
- Fe-Ni foil, Goodfellow Fe61/Ni39 (wt.%), 0.25 mm, measured purity 99.4 %

The materials were reduced before being placed into the ampoules. Firstly, the materials were weighed. The batch of the lead granules was first about 3 g but then decreased to about 2 g. This was due to the faster homogenization of the smaller sample. The batch for the foil was from 0.07

to 0.7 g, depending on the system under research. After weighing the material, it was placed into an Al_2O_3 crucible. The reduction was done overnight in a Lenton LTF 16/610 tube furnace in a 99.999 % hydrogen atmosphere. The reduction temperature was 523 K for lead and 1073 K for the metallic foils. After the reduction the samples were weighed again.

5.2 Experimental equipment

5.2.1 Quartz ampoules

Due to the high vapour pressure of lead, the experiments were conducted in quartz ampoules. This prevented lead loss during the experiments. Another benefit of the quartz ampoules was that the samples could be mixed during the experiments by turning the ampoules upside down. This helped to homogenize the alloys and accelerate diffusion.

The quartz ampoules used in the experiments were made of fused quartz glass under subcontract by Lasilaite Oy, Porvoo, Finland. The ampoule length was about 10 cm with a 1 cm outer diameter and 1 mm wall thickness. The ampoules were filled with argon, evacuated and sealed after filling the ampoules with the sample material. This prevented sample contamination with impurities such as oxygen. The pressure inside the ampoule was about 1 mbar. A neck was made in the middle of the ampoule in order to separate the liquid and solid material at the end of the experiment (see Figure 7).

5.2.2 Furnaces

The experiments for the binary systems were done with a Lenton UAF 16/10 laboratory chamber furnace with internal dimensions of a height of 190 mm, width of 180 mm, depth of 310 mm, silicon carbide elements and a Eurotherm control unit (Figure 5). Prior to the experiments, the hot zone of the furnace was determined at 873 and 1273 K, and it was found to be at the centre of the furnace. The quartz ampoules were standing upright next to the thermocouple on a sample holder made of ceramic fibre insulation sheet, which had a capacity of four ampoules per experiment. The sample holder was placed in the middle and at the bottom of the furnace. This was not the hottest part of the furnace but a compromise had to be made in order to build the sample holder so that the mixing of the ampoules could be done as quickly as possible. Nevertheless, the thermocouple was next to the quartz ampoules and molten lead, so that the actual equilibration temperature could be determined.

Figure 5. The equilibration experimental setup for the binary systems: a Lenton UAF 16/10 chamber furnace, S-type thermocouple, Keithley 2000 DMM, mercury thermometer and a PC for data logging.

The experiments for the ternary system were done with a vertical Lenton LTF 16/50/450 tube furnace with silicon carbide rod heating elements and a Eurotherm control unit. The alumina work tube dimensions were 1150 mm in length, an outer diameter of 55 mm and an inner diameter of 47 mm. The furnace was built on a special stand, with handles, which enabled the furnace to be turned by 180°, as shown in Figure 6. Prior to the experiments, the hot zone of the furnace was determined at 1273, 1373, 1473, 1573 K in order to find the right depth for the sample. The sample holder was gouged from ceramic fibre insulation sheet, integrated into the thermocouple protecting tube with Al_2O_3 mass, with the purpose of keeping the quartz ampoules hanging still from Pt wires without breaking during the experiment. The Pt wires were suspended by banana pins outside the work tube. A cooling cover with water pipes was attached to the furnace end mostly on top. One end of the work tube was closed with alumina wool and the other with a piece of ceramic fibre insulator and a metallic plate attached with butterfly nuts. Figure 6 shows the furnace and sample positions during the experiments (left) and immediately before quenching (right).

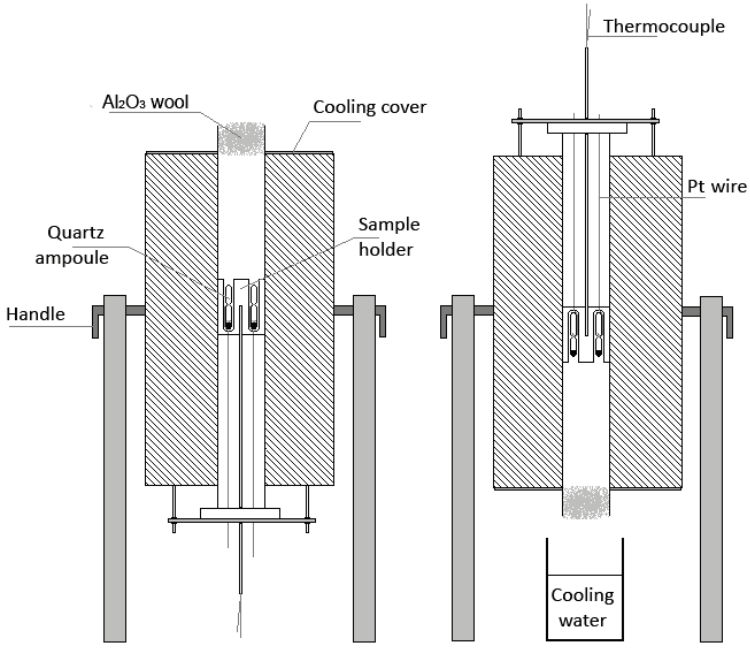

Figure 6. Lenton LTF 16/50/450 vertical tube furnace; on the left showing the furnace position during the experiment, and on the right prior to quenching. [IV]

5.2.3 Temperature measurement

Temperature measurement was made with a calibrated S-type (Pt-Pt10Rh) thermocouple, Keithley 2000 voltmeter and the NI LabVIEW temperature logging programme. The thermocouple was calibrated using the melting point of copper, later also against tin and iced water. The ambient temperature was measured with a mercury thermometer with an accuracy of ±0.1 K. This was changed later to a more accurate Pt100 sensor (Platinum Resistance Thermometer) from SKS Finland, and Keithley 2010 voltmeter. The manufacturer reported that the tolerance of the sensor was in accordance with DIN IEC 751 standard B1/10. The Pt100 sensor was calibrated against iced water at 273.15 K and the value was entered into the logging programme.

The uncertainty of the temperature measurement was calculated by expanded uncertainty with a coverage factor [66]:

$$U(t_v) = u(t_v) \cdot k = \left(\sqrt{u^2(\overline{q}_T) + u^2(\overline{q}_R) + u^2(\delta t_T) + u^2(\delta t_R) + \ldots} \right) \cdot k \qquad (34)$$

The uncertainty calculations took into account the standard deviation of the thermocouple reading, $u(q_T)$, the uncertainty of the room temperature measurement (in the case of a mercury thermometer), $u(q_R)$, the

corrections from the calibrations of the thermocouple, $u(\delta_T)$ and the room temperature measurement thermometer, $u(\delta_R)$. Also, the uncertainty caused by the insulator cover and the uncertainty caused by the mercury thermometer were taken into account in the case of the Fe-Pb system. The uncertainties were rounded up and multiplied with a coverage factor of k = 2.

5.3 Equilibration time

The equilibration time used in the equilibration experiments of iron, nickel, copper and iron-nickel with molten lead found in the literature ranged from tens of minutes [67] to a few hours [68-72] and up to 300 h [65], depending on the method and experimental temperature.

Pre-experiments on the equilibration time were conducted for the Ni-Pb binary system prior to the actual experiments. This was done by equilibrating solid nickel foil (Alfa Aesar Ni foil, 99.5 %, 0.1 mm) with liquid lead at 1273 K for different time periods of 4, 8, 16, 24, 32, 48, 96 h and analysing the change in liquid lead composition. The lead matrix with dissolved Ni was analysed using an ICP (Inductively Coupled Plasma) spectrometer. According to the pre-experiments, 48 h was thought to be more than enough for attaining equilibrium.

A theoretical study of the equilibration time was done for the Fe-Pb and Cu-Pb systems by calculating the diffusion coefficient in two ways: firstly, using the Arrhenius law by Robertson [73]; and secondly, using the Einstein-Sutherland equation by Borgstedt and Guminski [74]. The equations for calculating the diffusion coefficient of iron in lead, $D_{Fe/Pb,}$ are shown in [II] and that of copper in lead, $D_{Cu/Pb,}$ in [III].

The equilibration time for lead saturation in solid iron, nickel, copper and iron-nickel is somewhat poorly known and no attempt was made to measure these experimentally. It was assumed that a diffusion time of 48 h through the thin metallic foil would be enough to reach equilibrium. It was also assumed that the concentration profiles obtained by EPMA would reveal if equilibrium was not reached, in that they would show a clear parabolic shape indicating lower concentration in the middle of the sample. In [III], the diffusion coefficient of lead in copper, $D_{Pb/Cu,}$ was obtained from the publication of Prévot et al. [75] and calculated using the Arrhenius law. Based on this theoretical study, equilibration took less than a minute.

5.4 Experimental procedure

The quartz ampoules were set inside the chamber furnace in the sample holder next to the S-type thermocouple. After reaching the target temperature, the ampoules were turned upside down manually using tongs 48 times (6 x 8 turns) during the 48 h equilibration time in the furnace to

ensure homogeneity. The purpose of the neck in the middle of the ampoule was to separate the metallic foil (e.g. Fe foil) saturated with lead and the liquid lead saturated from the metallic foil, as shown in Figure 7 [II]. This was done by turning the ampoule 180° before quenching it in iced water. Firstly, an insulator cover was used around the ampoule in order to avoid breakage of the ampoule during turning due to heat or cold shock (the furnace door was open during the turning). Afterwards it was noticed that the ampoules managed to withstand the shocks without the cover and therefore the cover was not used any longer.

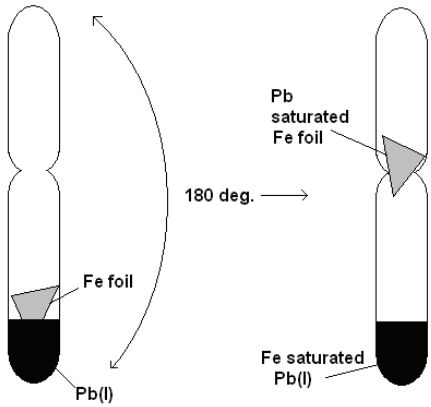

Figure 7. The quartz ampoule and the position of the samples (system Fe-Pb) inside the ampoule [II].

Later, for the ternary system experiments, the chamber furnace was replaced with a vertical tube furnace. In comparison to the earlier chamber furnace, the tube furnace allowed a more stable temperature to be maintained during the experiment. The whole furnace with the ampoules inside could be inverted, whereas in the chamber furnace the furnace door had to be opened. The ampoules were turned 50-60 times during the experiment. The tube furnace was considered safer to work with and quenching was slightly faster as the ampoule could be dropped straight into the cooling water under the furnace by releasing the Pt wire from the banana pin. On the other hand, it was not possible to see the samples during mixing with the tube furnace, as it had been with the chamber furnace.

After quenching, the ampoules were broken down and the compositions of saturated metals were analysed with ICP and EPMA (Electron Probe

Microanalysis). Table 1 shows a summary of the parameters related to the experiments.

Table 1. Summary of the experimental parameters.

	Fe-Pb	Cu-Pb	Ni-Pb	Fe-Ni-Pb
Furnace type	Chamber	Chamber	Chamber	Vertical tube
Thermocouple calibration	Cu	Cu	Cu	Cu, Sn, iced water
Room temperature	Hg thermometer	Pt100	Pt100	Pt100
Temperature uncert. [K]	4.8	3.6	7.1	3.7
Insulator cover	Yes	No	No	No
Mass of lead granules [g]	3	2	2	2
Mass of metallic foil [g]	0.07	0.6	0.3 - 0.4	0.6 - 0.7
Equilibration time [h]	48	48	48	48
Mixing times (minimum)	48	48	48	50-60
Temperature range [K]	1371.2 - 1571.1	866.3 - 1166.4	1259.3 - 1512.2	1283.1 - 1530.3
ICP analysis	NN*	BOHA**	NN*	ORC***

* Norilsk Nickel Harjavalta Oy, ** Boliden Harjavalta, *** Outotec (Finland) Oy, Research Center

5.5 Chemical analysis equipment

5.5.1 Inductively Coupled Plasma Spectrometer

The lead matrices with dissolved metal were analysed by Inductively Coupled Plasma (ICP) spectrometer, which is a chemical analytical method where plasma is used as atomizer. The samples were dissolved with acidic media and dissolved with diluted water prior to analysis. During analysis, the sample is atomized into atoms or elementary ions and the species are excited to higher electronic states. After the excitation the species go back to the lower states, which can be detected as ultraviolet and visible line spectra. This information can be used in quantitative and qualitative elemental analyses. [76]

The ICP analyses conducted in this work were carried at different companies involved in the ISS project and the equipment used for specific samples is reported in [II-IV]. The companies have accredited analysis services and the uncertainties of the analyses were received from the companies along with the analysis. The uncertainties were calculated based on standard deviations of the equipment performance and sample preparation with a confidence level of 95 % (k=2).

5.5.2 Scanning Electron Microscope

Scanning Electron Microscope (SEM) gives physical data concerning the surface of the sample, such as morphology, that is similar to those accessed by the human eye. In this technique, the surface of the sample is bombarded with an electron beam. The obtained signal is stored in a computer where it is converted into an image. The signal can be backscattered, secondary or Auger electrons, X-ray fluorescence photons or other photons of various energies. [76]

For chemical analysis, an X-ray detector is needed and Energy Dispersive Spectrometry (EDS) is used for this purpose [76]. With the combination of

SEM-EDS, it is possible to obtain both surface images showing the homogeneity and chemical analysis of the samples.

SEM-EDS was used to analyse the purity of the commercial Fe-Ni foil. The equipment used within this work was an Oxford Instruments Leo 1450 with an Oxford Instruments X-Max 50mm2 EDS detector by the Department of Materials Science and Engineering, Aalto University. The standards were nickel 99.97 % wire (Alfa Aesar) and iron 99.995 % wire (Alfa Aesar) from SPI Supplies. For both standards the Kα peak was used. The accelerating voltage was 15 kV and the spot size 460 nm.

5.5.3 Electron Microprobe Analysis

The metallic foil saturated with lead was prepared for electron probe microanalysis (EPMA) by the Geological Survey of Finland (GTK). EPMA is a scanning electron microscope with wavelength dispersive spectrometers (WDS) attached. Electron probe microanalysis enables the determination of the elemental composition of surfaces. In this technique, the surface of the sample is bombarded with a focused beam of high-energy electrons in the SEM to impinge on a sample to induce emission of characteristic X-ray from each element. The X-ray fluorescence photons from the sample are collimated, dispersed by a single crystal, detected and analysed. Both qualitative and quantitative information is obtained about the surface of the sample. [11,76]

The EPMA equipment used in this study was a Cameca SX 100 EPMA and was used to analyse trace elements. The EPMA analysis parameters are reported in [II-IV]. The uncertainties of the EPMA analyses were calculated with standard deviation from the mean of the measurement points. In publication [IV] the uncertainty originating from the equipment was also taken into account by measuring ten points exactly from the same spot of the sample (i.e. the same coordinates). Thus, the overall uncertainty of the EPMA analysis contained the standard deviations of the profile points and a ten-point analysis.

6. Results and discussion

Due to the fact that the optimization of the thermodynamic model parameters is based on experimental data, it is crucial that accurate experimental data exist in order to create reliable CALPHAD assessments and thermodynamic databases. However, research groups performing experiments are becoming fewer and fewer because experiments tend to be expensive and time-consuming, modelling being thus faster and more economical. Nevertheless, the model is only as accurate as the experimental data used in the assessment and therefore experiments are needed as an important part of CALPHAD assessments and validation of the models. The aim of this work was to extend the thermodynamic MTOX database with the [Cu,Fe,Ni]-Pb binary and Fe-Ni-Pb ternary systems. The results obtained within this work are presented in Appendices [I-V], but a summary with discussion is given below. The figures and the references in the figures presented in Sections 6.2 and 6.3 can be found in Appendices [I-V].

6.1 Equilibration experiments

All the lead alloy systems investigated were previously known to some extent, which made it easier to start the experiments. Although the experimental method might appear simple, there were challenges to overcome and several uncertainty factors were perceived. The method was developed continuously in order to obtain as accurate results as possible.

Firstly, the room temperature measurement that was in principle taken with a mercury thermometer was changed to a Pt100 resistance thermometer. This made it possible to obtain more accurate temperature measurement and eased the analysis of the temperature logging data.

The insulation covers used around the quartz ampoules were found to be redundant, because the ampoules could withstand the heat and cold shocks resulting from the mixing of the samples.

The test materials were reduced in a hydrogen atmosphere to remove the oxygen layer of the metals. It is possible that some residual oxygen and hydrogen were present during the experiments. However, at room

temperature the solubility of hydrogen and oxygen in iron, nickel and copper is very low [91]. Even though care was taken when dispatching the test materials, the author did not make the ampoules herself.

Maintaining a stable temperature during the experiments was an issue, because the chamber furnace door had to be opened for sample mixing. This also had an impact on the calculated temperature measurement uncertainty. Eventually this led to the development of a vertical tube furnace [IV], which was also more comfortable to work with.

With the tube furnace, sample quenching was slightly faster compared to the chamber furnace. Quartz has a rather low thermal conductivity, which probably decelerated quenching. No attempt was made to use any other quenching media such as liquid nitrogen. Additionally, the experimental results obtained with the current technique showed similar values to those obtained with other techniques in the literature.

During the experiments, part of the metal foil was not in contact with the liquid lead, as shown in Figure 7. The sample preparation was done in such a way that grinding was started from the tip of the foil in contact with the lead to make sure that the EPMA analysis was obtained from the foil part equilibrated with the lead.

During quenching, some of the remaining non-dissolved lead was attached to the surface of the foil. This posed a challenge for EPMA analysis, because soft lead might have some influence during grinding and polishing, spreading from the outer surface of the foil to the cross-section of the sample. The analysis points were selected to avoid parts where lead was observed, but the absence of spread lead could not be guaranteed.

As mentioned earlier in Section 5.3, the equilibration time for lead saturation in solid iron, nickel, copper and iron-nickel was not measured experimentally. It was assumed that the diffusion time of 48 h through the thin metallic foil was enough to reach equilibrium. It was also assumed that the concentration profiles obtained by EPMA would reveal if equilibrium was not reached in that they would show a clear parabolic shape indicating lower concentration in the middle of the sample. Nevertheless, no composition gradients that would indicate incomplete equilibrium were observed. However, it would be worth determining the saturation of lead in these metals experimentally in the future.

6.2 Thermodynamic (re-)assessments

The literature compilations done for the lead-alloy assessments aim to cover all the published data from the early 20th century until today. The systems were assessed with MTDATA software using critically selected data from the literature and from our own equilibration experiments.

The selection of a solution model depends on the crystal structure of the phase and on how easily the description of binary data can be combined with other binary systems for the calculation of higher-order systems [64]. In database development, the thermodynamic models used need to be compatible with the rest of the database. As the lead systems assessed in this work are simple, with no intermediate phases and no chemical ordering, a simple substitutional model was used. The model describes the non-ideal interactions of the system components with the Redlich-Kister polynomial. The same model was used in the Ni-Pb [77,78], Cu-Pb [77,79-81] and Fe-Pb [82-84] assessments reported in the literature. For pure elements, the SGTE Unary data were used. Both the SGTE Unary database for pure elements and the Redlich-Kister polynomial for the solution phases are compatible with the MTOX database. The experimental data were fitted by a least squares method. All the modelled binary systems consisted of a large liquid miscibility gap with very little mutual solubility in each other and with no intermediate phases, and no chemical ordering. Consequently, they were quite simple systems to model. The Fe-Ni binary system forms order-disorder phases at low temperatures [85], but these are not described in the MTOX database from which the Fe-Ni thermodynamic parameters were taken.

6.2.1 The Ni-Pb system

Publication [I] was the beginning of the lead alloy database development work. We had no experimental results of our own at that time to be included in the assessment. A data compilation and critical evaluation were made, on the basis of which it was noticed that the Ni-rich end was poorly known experimentally and the value of lead solid solubility in nickel by Voss of 1.2% (extrapolated) [86] or Pomianek of 0.9 % (calculated) [87] were not directly measured values. Also, new experimental data of the lead-rich end below the eutectic temperature by Amenzou-Badrour et al. [88] were found. These data had not been used in the Ni-Pb assessments before and therefore made it possible to obtain a more accurate description of the nickel solid solubility in lead, the eutectic point at the lead-rich end and nickel solubility above the eutectic temperature, as shown in Figure 8.

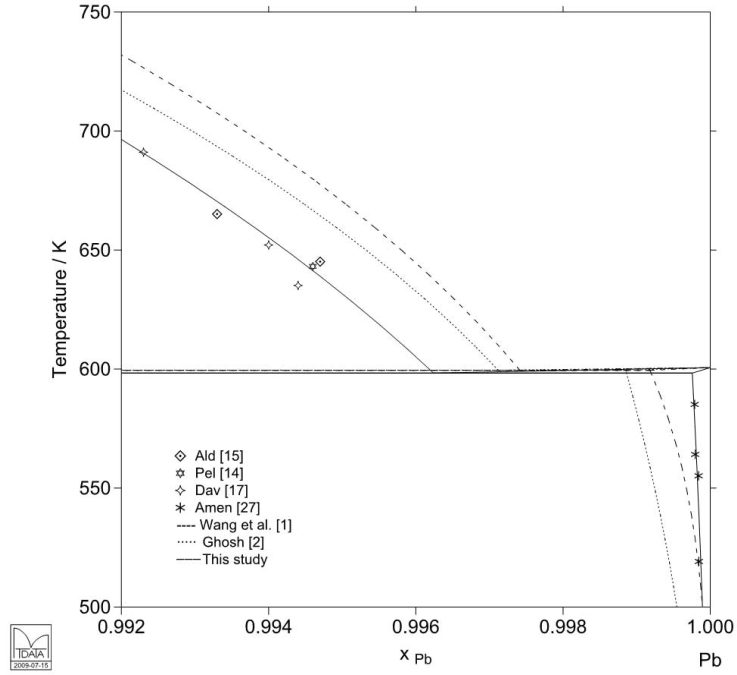

Figure 8. The calculated Pb-rich end of the Ni-Pb phase diagram based on the parameter sets reported in [I] and [77,78] with experimental data superimposed. The figure is reproduced from [I].

Later, the Ni-rich side could be described more accurately in [IV], where the mutual solubilities at 1260 – 1510 K were determined experimentally. The measured solubilities at the lead-rich end were in agreement with the literature data, except at 1359.7 K, which showed a greater solubility (see [IV], Figure 6). The reason for this could be an analytical error. However, the calculated liquidus curve at the lead-rich end is in good agreement with the experimental data.

Compared to the calculated phase diagrams based on the parameter set in [I], the nickel solubility in lead below the eutectic temperature remained the same and was slightly smaller above the eutectic temperature but still in good agreement with the experimental data (see [IV], Figure 8).

Figure 9 shows the maximum solid solubility of lead in nickel at the monotectic temperature, which was found to be slightly bigger than that calculated with the parameter sets from [77,78] and [I].

The calculated critical point of the liquid phase miscibility gap was calculated to be at a lower temperature than reported earlier by Miller and Elliot [68]. It was noticed that their three topmost points of [68] were estimated and not directly measured values, thus, the calculated lower value was realistic.

Even though the Ni-Pb phase diagram is rather well known, experimental data of the liquid miscibility gap is needed to improve the thermodynamic description of the system. Measurement of liquid immiscibility is challenging but could be done by, for example, high temperature mass spectrometry by measuring the activity of lead in a Ni-Pb alloy.

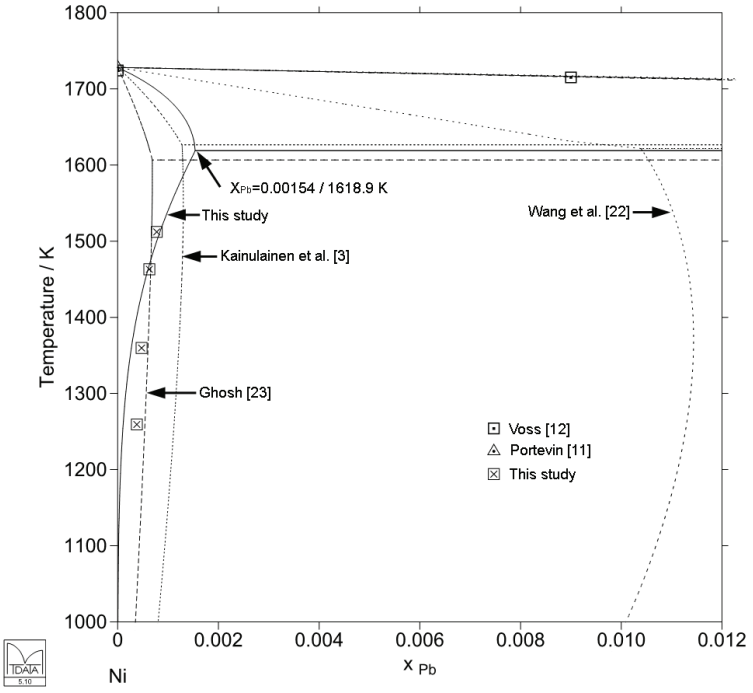

Figure 9. The calculated Ni-rich end of the Ni-Pb phase diagram based on the parameter sets reported in [I,IV] and [77,78] with experimental data superimposed. The figure is reproduced from [IV]. "Kainulainen et al. [3]" refers to Publication [I].

6.2.2 The Fe-Pb system

After data compilation, it was noticed that the Fe-Pb system is not well known and that only experimental phase diagram data are available in the literature. Even though it would have been favourable to improve the thermodynamic description with thermodynamic data, nevertheless the experimental data reported in [II] gave a valuable contribution to the scarce amount of data existing.

Some confusion was noticed with the atomic and weight fractions in the previous thermodynamic assessments by Onderka et al. [82] and Hämäläinen et al. [84], which were corrected in this work.

The equilibration experimental results reported in [II] showed a very limited solid solubility at the iron-rich end, below the monotectic temperature. Also, the results were scattered, which was believed to be due to non-dissolved lead around the iron foil sample. The calculated phase

diagram of the Fe-rich end is in good agreement with the experimental points, as shown in Figure 10.

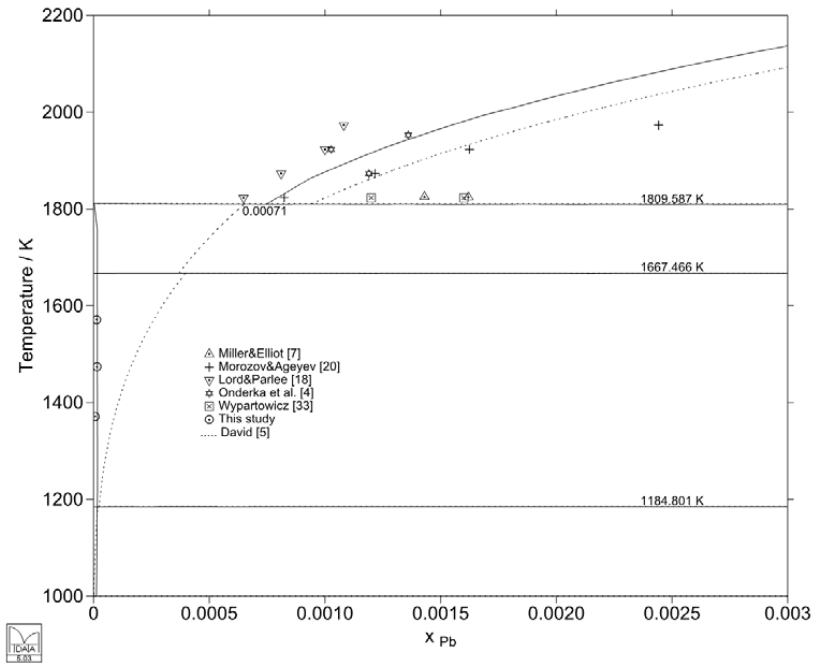

Figure 10. The calculated Fe-rich end of the Fe-Pb phase diagram based on the parameter sets reported in [II] and [83] with experimental data superimposed. The figure is reproduced from [II].

The experimental results at the lead-rich end were in fairly good agreement with the other experimental data reported previously in the literature ([II], Figure 4). However, the calculated liquidus curve could be in better agreement with our own experimental data at higher temperatures. The calculated liquidus agrees very well with the experimental liquidus data reported by [89], which were considered very reliable in the critical assessment [II].

Nevertheless, with the new and slightly different experimental data than that used in the assessment by Onderka et al. [82] and Hämäläinen et al. [84], the thermodynamic description is improved. In order to further improve the description, more experimental thermodynamic data are required. Also, experimental data of the liquid miscibility gap would be necessary but it is extremely challenging to conduct such experiments due to the very high temperatures involved.

6.2.3 The Cu-Pb system

The Cu-Pb binary system is the most well known of the systems covered in this thesis. Phase diagram and thermodynamic data of the system exist and

the liquid miscibility gap has been measured by several authors. The thermodynamic assessment has been published previously by [77,79-81] and Vaajamo et al. [90], as a part of our Cu-Fe-Pb assessment. There were no experimental results of our own at that time to be included in the assessment. But it was noticed, as in all the previous systems, that the solubility of lead in solid copper was unknown. One experimental point exists by Raub and Engel [92], and according to them “the solubility is not more than 0.09 at.% Pb”. Also, some older experimental data on copper solubility in solid lead below the eutectic temperature were found in the literature, which had not been used in the previous assessments.

This new critically selected literature data and data from our own experiments were used to re-assess the Cu-Pb system FCC_A1 phase interaction parameters. The experimentally determined liquidus points were used to validate the calculated liquidus curve based on the parameter set in [90], and showed good agreement with the calculated liquidus curve (see [III], Figure 4).

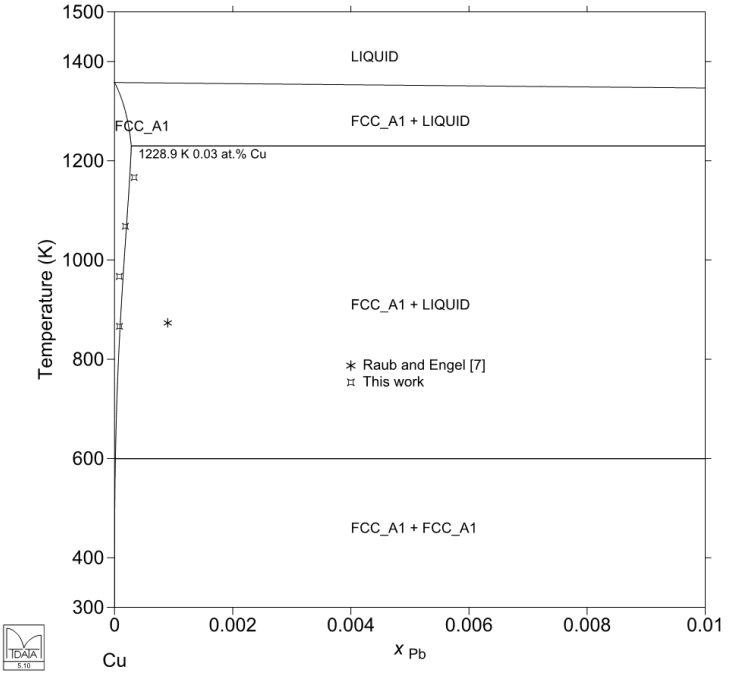

Figure 11. The calculated Cu-rich end of the Cu-Pb phase diagram based on the parameters sets reported in [III] with the experimental data superimposed. The figure is reproduced from [III].

The solvus curve at the lead-rich end shows very good agreement with the experimental data (see [III], Figure 3). According to the study in [III], the solubility of lead in solid copper is smaller than the experimental point reported by Raub and Engel [92]. This is presented in Figure 11. The

thermodynamic description of the Cu-Pb system has been improved in the area of FCC_A1 solid solution.

6.2.4 The Fe-Ni-Pb system

The Fe-Ni-Pb ternary system has not been assessed previously, and in this work the interaction parameters of the ternary liquid phase were optimized. The experimental results obtained in [IV] diverged from the values by Fleischer and Elliot [69], which also showed discrepancies with each other. Thus, their [69] values were ignored in this optimization.

Xiong et al. [59] proposed that the lattice stability of Ni in the SGTE pure element compilation needed revision. They also reported [59] that the conventional Redlich-Kister polynomial is not sufficient to describe the Fe-Ni magnetic phase diagram. The thermodynamic data for pure nickel was taken from the SGTE Unary database without any modifications and the Fe-Ni interaction data was taken from the MTOX database, which uses the Inden-Hillert-Jarl model [57,58] to describe the magnetic contribution and does not consider any low temperature chemical ordering. Another thermodynamic assessment could have been made of the Fe-Ni-Pb ternary system using a 4-sublattice model with the purpose of introducing the order-disorder phases at low temperatures, but no practical benefits could be seen, so this was left for the future work of other researchers.

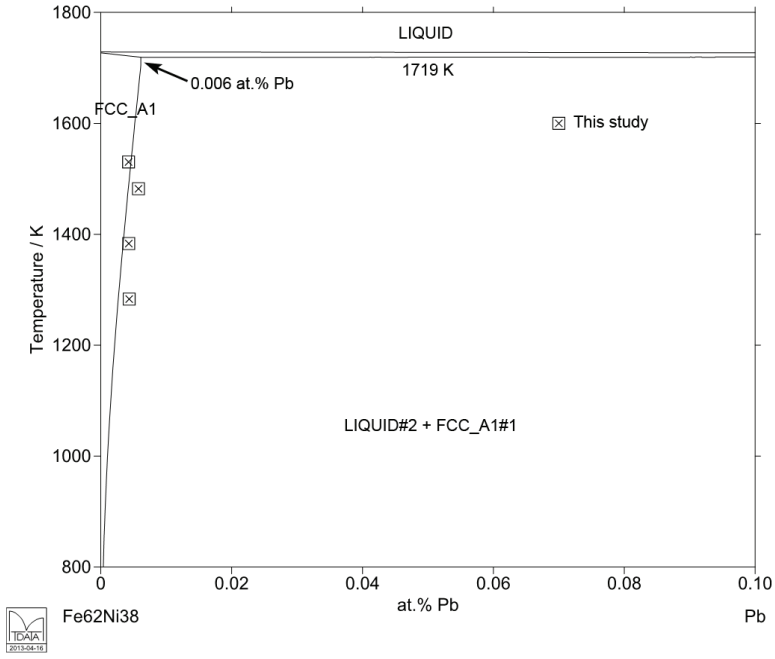

Figure 12. A calculated temperature-composition section starting from $Fe_{62}Ni_{38}$ (at.%) and covering additions of up to 0.1 at.% Pb with experimental data superimposed. The figure is reproduced from [IV].

According to the experimental results, the solid solubility of lead in Fe-Ni (61 wt.% Fe, 39 wt.% Ni) foil is small and does not change much as a function of temperature, as can be seen in Figure 12.

The overall agreement of the calculated phase diagrams with the experimental data is good and the assessment is valid above the magnetic transition temperatures.

As the experimental phase diagram data of the ternary system is limited, in the future the thermodynamic description of the system could be improved with new experimental thermodynamic data.

6.3 From theory to practice

The ultimate goal of the equilibration experiments and thermodynamic assessments conducted within this thesis is that they would serve those parties who deal with practical problems and who could use them in solving material engineering related problems. Publication [V] was written as a compilation of the work of this thesis with some practical cases containing the current coverage of the MTOX database, with new viscosity and electrical conductivity models, and an illustrative example of an electric slag cleaning furnace. Figure 13 illustrates the lead fraction in slag (OXIDE_LIQUID), metal (LIQUID) and gas phases during the electric furnace slag cleaning process [V] when the weight fraction of ferric oxide is reduced from the slag by a suitable reducing agent such as coke.

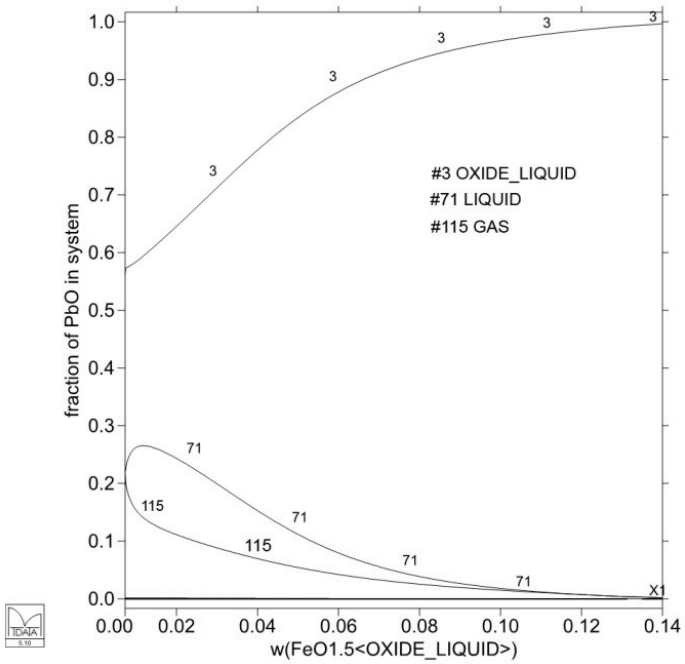

Figure 13. The calculated lead fractions in the slag (#3), metal (#71) and gas (#115) phases as a function of slag reduction rate. The figure is reproduced from [V].

Publication [V] is intended to show the extensive coverage of the MTOX database and illustrate the types of problems that can be solved using it. As thermodynamics is sometimes considered nebulous, it is necessary to introduce this kind of compilation contribution to show the importance of thermodynamics and its use in real life.

6.4 Future work

It is important to make experiments and even to reproduce reported data and accordingly confirm earlier experimental data. This can also minimize the errors coming from the experiments. This is also the way to obtain (more) accurate thermodynamic descriptions of the systems of interest, and consequently full benefit of the thermodynamic databases in practice. Even one experimental point from an unknown part of the phase diagram could improve its accuracy significantly. Therefore, more experimental data, results from quantum mechanical calculations and thermodynamic data, which is often lacking, should be produced for the future, rather than phase diagram data.

The database developed in this work is rather narrow as such and it should be expanded with other lead-based systems in order to extract its full potential. This has been done in some other publications by the author [24-26,90] and possibly the work will continue in the near future.

7. Conclusions

The CALPHAD method is a powerful tool in materials science and metallurgy but in order to use it in practical applications, it is necessary to build multicomponent databases that contain thermodynamic data of binary, ternary and higher order systems. Building a database begins with a uniform set of pure elements and reliably assessed lower-order systems, continuing to a higher-order system.

Experiments are a crucial part of the CALPHAD assessment required for the parameter optimization and validation of the modelled system, as the model is only as accurate as the experimental data used in the assessment. There are more scientists making assessments today than conducting experimental measurements. Even one accurate experimental point from a previously unknown area provides a valuable contribution to the thermodynamic description of the system. It is also important to reproduce reported data and accordingly confirm earlier experimental data.

In this work, the objective was to extend the MTOX thermodynamic database with the following lead alloy systems: Ni-Pb, Fe-Pb, Cu-Pb and Fe-Ni-Pb, using data from the literature and from our own isothermal equilibration experiments. With the experimental method, the mutual solubilities of liquid lead and solid metal foil (Fe, Cu, Ni or Fe-Ni) were measured isothermally in a quartz ampoule over a certain temperature range. The compositions of the alloys were analysed with an ICP spectrometer and by EPMA. The solubility of lead in these solid metals was not known previously, except for one rather inaccurate temperature-composition point of the Cu-Pb system. According to the results, the lead solid solubility in the metallic foils was the smallest in iron, then in iron-nickel, nickel, and the greatest in copper. The same order was valid also when measuring metal solubilities in molten lead: iron dissolved the least, then iron-nickel, then nickel, and copper the most. The lead solid solubilities obtained in this thesis tended to be smaller than those reported previously in the literature [92] or in the thermodynamic assessments. The solubilities in the molten lead alloys were in agreement with previously published experimental literature data.

The experimental method used within this work was developed continuously in order to obtain as accurate data as possible. There are still issues to be improved but as the world is as it is, a measurement point will always have a measurement uncertainty.

The lead alloy systems were assessed with MTDATA software, in its Assessment module, using data from the literature and from our own equilibration experiments. The SGTE Unary data was used for pure elements and non-ideal solution phases were described with the Redlich-Kister polynomial. These are compatible with the MTOX database of NPL. The experimental data were fitted by a least squares method. As a conclusion of the thermodynamic assessments, it can be stated that the agreement of the calculated phase equilibria with the critically evaluated and selected experimental points was good and that the thermodynamic descriptions of these systems have been improved.

The lead alloy database serves as a basis for further development work if/when new experimental data are produced. For the moment, these lead alloy assessments together with the MTOX database can be used in calculating the thermodynamic properties and phase equilibria of large industrial multicomponent systems.

8. References

1. M. Oguchi, H. Sakanakura, A. Terazono, “Toxic metals in WEEE: Characterization and substance flow analysis in waste treatment processes,” Science of the Total Environment (2012). In press.
2. M.E. Schlesinger, M.J. King, K.C. Sole, W.G. Davenport, Extractive metallurgy of copper, 5th ed. Oxford, UK: Elsevier Ltd, 2011.
3. T. Norgate, S. Jahanshahi, “Low grade ores – Smelt, leach or concentrate?,” Minerals Engineering 23 (2010) 65-73.
4. P. Swart, J. Dewulf, “Quantifying the impacts of primary metal resource use in life cycle assessment based on recent mining data,” Resources, Conservation and Recycling 73 (2013) 180-187.
5. K. Nakajima, O. Takeda, T. Miki, T. Nagasaka, “Evaluation method of metal resource recyclability based on thermodynamic analysis,” Materials Transactions 50 (2009) 3, 453-460.
6. L. Kaufman, H. Bernstein, Computer calculation of phase diagrams with special reference to refractory metals. J.L. Margrave (Ed.), New York, USA: Academic Press, Vol. 4, 1970.
7. N. Saunders, A.P. Miodownik, CALPHAD (Calculation of phase diagrams) A comprehensive guide. R.W. Cahn (Ed.), Oxford, UK: Pergamon, Elsevier Science Ltd, Vol. 1, 1998.
8. H.L. Lukas, S.G. Fries, B. Sundman, Computational thermodynamics, the Calphad method. Cambridge, UK: Cambridge University Press, 2007.
9. J.A. Gisby, A.T. Dinsdale, I. Barton-Jones, A. Gibbon, P. Taskinen, “Predicting phase equilibria in oxide and sulphide systems.” In: Proceedings of the European Metallurgical Conference (EMC), 2007 June 11-14, Düsseldorf, Germany. GDMB Medienverlag, Clausthal-Zellerfeld, Germany; 2007, Vol. 4, pp. 1721-1736.
10. P. Taskinen, A. Dinsdale, J. Gisby, “Industrial slag chemistry: a case study of computational thermodynamics,” Scandinavian Journal of Metallurgy 34 (2005) 100-107.
11. J.-C. Zhao (Ed.) Methods for phase diagram determination. Oxford, UK: Elsevier Ltd, 2007.
12. R.H. Davies, A.T. Dinsdale, J.A. Gisby, J.A.J. Robinson, S.M. Martin, “MTDATA-thermodynamic and phase equilibrium software from the National Physical Laboratory,” CALPHAD 26 (2002) 2, 229-271.

13. U.R. Kattner, P.J. Spencer, G. Eriksson, T.J. Anderson et al. “Workshop on applications of computational thermodynamics: Schloβ Ringberg, November 30–December 5, 1997,” CALPHAD 24 (2000) 1, 55-94.
14. J. Ågren, F.H. Hayes, L. Höglund, U.R. Kattner, B. Legendre, R. Schmid-Fetzer, “Applications of computational thermodynamics,” Zeitschrift für Metallkunde 93 (2002) 2, 128-142.
15. M.G. King, “The evolution of technology for extractive metallurgy over the last 50 years—Is the best yet to come?,” JOM 59 (2007) 2, 21-27.
16. I. Jung, “Overview of the applications of thermodynamic databases to steelmaking processes,” CALPHAD 34 (2010) 332-362.
17. V. Laporte, A. Mortensen, “Intermediate temperature embrittlement of copper alloys,” International Materials Reviews 54 (2009) 2, 94-116.
18. A. Dinsdale, A. Watson, A. Kroupa, J. Vřešťál, A. Zemanová, J. Vízdal, COST 531 Lead free solders, Atlas of phase diagrams for lead-free soldering. Brussels, Belgium: COST Office, Vol.1, 2008.
19. S. Guruswamy, Engineering properties and applications of lead alloys. New York, USA: Marcel Dekker, 2000.
20. V. Sobolev, “Thermophysical properties of lead and lead-bismuth eutectic,” Journal of Nuclear Materials 362 (2007) 235-247.
21. K. Nakajima, O. Takeda, T. Miki, K. Matsubae, T. Nagasaka, “Thermodynamic analysis for the controllability of elements in the recycling process of metals,” Environmental Science & Technology 45 (2011) 4929-4936.
22. C. Hassall, H. Roberts, “Worldwide lead supply and demand.” In: A. Siegmund, L. Centomo, C. Geenen, N. Piret, G. Richards, R. Stephens (Eds.) Proceedings of the Lead-Zinc Conference (PbZn), 2010, October 3-6, Vancouver, Canada. Wiley, New Jersey, USA; 2010, pp. 17-25.
23. K. Yamaguchi, Y. Takeda, “Impurity removal from carbon saturated liquid iron using lead solvent,” Materials Transactions 44 (2003) 12, 2452-2455.
24. I. Vaajamo, P. Taskinen, ”A Thermodynamic Assessment of the Co-Ni-Pb Ternary System.” In: Proceedings of the Thermodynamics of Alloys (TOFA) 2010, September 12-17, Porto, Portugal. ISBN: 978-972-752-126-5. In Press in FEUP Edições, http://feupedicoes.fe.up.pt/index.php

25. I. Vaajamo, “A thermodynamic assessment of the X-Pb (X=Co,Cr,Ni,Fe) binary systems,” Licentiate thesis, Aalto University, Finland, 2011.
26. I. Vaajamo, P. Taskinen, “Thermodynamic assessments of the [Co,Cr,Fe,Ni]-Pb binary systems.” In: Book of abstracts of CALPHAD XL, 2011, May 22th - 27, Rio de Janeiro, Brazil. Associação Brasileira de Metalurgia, Materiais e Mineração, Sao Paolo, Brazil; 2011, p. 159.
27. A. Pelton, Thermodynamics and phase diagrams of materials. R.W. Cahn, P. Haasen, E.J. Kramer (Eds.), Materials science and technology, Phase transformations in materials. Weinheim, Germany: VCH, 1991, Vol. 5, pp. 1-73.
28. P.J. Spencer, “A brief history of CALPHAD,” CALPHAD 32 (2008) 1-8.
29. A. Costa e Silva, J. Ågren, M.T. Clavaguera-Mora, D. Djurovic, T. Gomez-Acebo, B.-J. Lee, Z.-K. Lui et al., “Applications of computational thermodynamics – the extension from phase equilibrium to phase transformations and other properties,” CALPHAD 31 (2007) 53-74.
30. A. Kroupa, “Modelling of phase diagrams and thermodynamic properties using Calphad method – Development of thermodynamic databases,” Computational Materials Science 66 (2013) 3-13.
31. U.R. Kattner, “The thermodynamic modeling of multicomponent phase equilibria,” JOM 49 (1997) 12, 14-19.
32. J.-O. Andersson, T. Helander, L. Höglund, P. Shi, B. Sundman, “Thermo-Calc & DICTRA, computational tools for materials science,” CALPHAD 26 (2002) 2, 273–312.
33. C.W. Bale, P. Chartrand, S.A. Degterov, G. Eriksson, K. Hack, R. Ben Mahfoud, J. Melançon et al., “FactSage thermochemical software and databases,” CALPHAD 26 (2002) 2, 189–228.
34. A.T. Dinsdale, “SGTE data for pure elements,” CALPHAD 15 (1991) 4, 317-425.
35. L.A. Cornish, R. Süss, A. Watson, S.N. Prins, “Building a thermodynamic database for platinum-based superalloys: Part I,” Platinum Metals Review 51 (2007) 3, 104-115.
36. A. Watson, R. Süss, L.A. Cornish, “Building a thermodynamic database for platinum-based superalloys: Part II,” Platinum Metals Review 51 (2007) 4, 189-198.
37. N. Dupin, I. Ansara, C. Servant, C. Toffolon, C. Lemaignan, J.C. Brachet, “ A thermodynamic database for zirconium alloys,” Journal of Nuclear Materials 275 (1999) 287-295.

38. K. Hack (Ed.), The SGTE casebook, Thermodynamics at work. London, UK: The Institute of Metals, 1996.
39. M. Hillert, “Thermodynamic modelling of solutions,” CALPHAD 21 (1997) 2, 143-153.
40. I. Ansara, “Comparison of methods for thermodynamic calculation of phase diagrams,” International Metals Reviews 24 (1979) 1, 20-53.
41. F.D. Murnaghan, “The compressibility of media under extreme pressures,” Proceedings of the National Academy of Sciences of the United States of America 30 (1944) 9, 244-247.
42. I. Barin, Thermochemical data of pure substances, Part I. Weinheim, Germany: VCH, 1989.
43. K.K. Kelley, “Contributions to the data on theoretical metallurgy: X.” Bureau of Mines, U.S. Government Printing Office, Washington, D.C.; 1949, No. 476.
44. O. Redlich, T. Kister, “Algebraic representation of thermodynamic properties and the classification of solutions,” Industrial & Engineering Chemistry 40 (1948) 2, 345-348.
45. I. Ansara, “The representation of thermodynamic properties in multicomponent alloys,” Materials Research Society Symposium Proceedings 19 (1983) 107-114.
46. M. Margules, “Über die zusammensetzung der gesättigten dämpfe von mischungen,” Sitzungsberichte der Kaiserliche Akadamie der Wissenschaften Wien Mathematisch-Naturwissenschaftliche Klasse, Wien, 104 (1895) 1243-1278.
47. C.W. Bale, A.D. Pelton, “Mathematical representation of thermodynamic properties in binary systems and solutions of Gibbs-Duhem equation,” Metallurgical Transactions 5 (1974) 2323-2337.
48. O. Redlich, Thermodynamics: Fundamentals, applications. Amsterdam, The Netherlands: Elsevier, 1976.
49. I. Ansara, C. Bernard, L. Kaufman, P. Spencer, “A comparison of calculated phase equilibria in selected ternary alloy systems using thermodynamic values derived from different models,” CALPHAD 2 (1978) 1, 1-15.
50. M. Hillert, “Empirical methods of predicting and representing thermodynamic properties of ternary solution phases,” CALPHAD 4 (1980) 1, 1-12.
51. P. Chartrand, A.D. Pelton, “On the choice of “geometric” thermodynamic models,” Journal of Phase Equilibria 21 (2000) 2, 141-147.

52. A.D. Pelton, “A general “geometric” thermodynamic model for multicomponent solutions,” CALPHAD 25 (2001) 2, 319-328.
53. F. Kohler, “Zur berechnung der thermodynamischen daten eines ternären systems aus den zugehörigen binären systemen,” Monatshefte für Chemie 91 (1960) 4, 738-740.
54. G.W. Toop, “Predicting ternary activities using binary data,” Transactions of the Metallurgical Society of AIME 233 (1965) 850-854.
55. Y.-M. Muggianu, M. Gambino, J.-P. Bros, “Enthalpies de formation des alliages liquides bismuth-étain-gallium a 723 K. Choix d’une représentation analytique des grandeurs d’excès intégrales et partielles de mélange,” Journal de Chimie Physique 72 (1975) 1, 83-88.
56. H.M. Lee, “Interaction parameters of lead-base ternary system,” CALPHAD 16 (1992) 1, 47-52.
57. G. Inden, “Approximate description of the configurational specific heat during a magnetic order-disorder transformation.” In: Proceedings of the 5th CALPHAD Conference, 1976. Max-Planck-Institut für Eisenforschung, Düsseldorf, Germany; 1976, III, pp. 1-13.
58. M. Hillert, M. Jarl, “A model for alloying effects in ferromagnetic metals,” CALPHAD 2 (1978) 3, 227-238.
59. W. Xiong, H. Zhang, L. Vitos, M. Selleby, “Magnetic phase diagram of the Fe-Ni system,” Acta Materialia 59 (2011) 521-530.
60. W. Xiong, Q. Chen, P.A. Korzhavyi, M. Selleby, “An improved magnetic model for thermodynamic modeling,” CALPHAD 39 (2012) 11-20.
61. D. Lindberg, “Thermochemistry and melting properties of alkali salt mixtures in black liquor conversion processes,” Doctoral thesis, Åbo Akademi University, Finland, 2007.
62. C. Robelin, “Models for the thermodynamic properties and physical properties (density, viscosity, electrical conductivity) of molten salts of industrial interest,” Chemical Thermodynamics in Furnaces – A joint symposium and course for combustion specialists and metallurgists, 2012 January 30-February 3, Åbo Akademi University, Turku, Finland.
63. P.E.A. Turchi, I.A. Abrikosov, B. Burton, S.G. Fries, G. Grimvall, L. Kaufman et al., ”Interface between quantum-mechanical-based approaches, experiments, and CALPHAD methodology,” CALPHAD 31 (2007) 4-27.

64. R. Schmid-Fetzer, D. Andersson, P.Y. Chevalier, L. Eleno, O. Fabrichnaya, U.R. Kattner et al., “Assessment techniques, database design and software facilities for thermodynamics and diffusion,” CALPHAD 31 (2007) 38-52.
65. O.J. Kleppa, J.A. Weil, “The solubility of copper in liquid lead below 950°,” Journal of the American Chemical Society 73 (1951) 10, 4848-4850.
66. T. Weckström, “Lämpötilan mittaus,” MIKES (Centre for Metrology and Accreditation) publication, 2005. p. 138. (In Finnish) Available: http://www.mikes.fi/documents/upload/j4_05_www.pdf (cited 4.7.2013)
67. T.R.A. Davey, “Determination of solubilities in liquid metals.” In: G.R. St. Pierre (Ed.) Proceedings of the Metallurgical Society Conferences, Physical Chemistry of Process Metallurgy, Part 1, 1959 April 27-May 1, Pittsburgh, USA. Interscience Publishers, New York, USA; 1961, Vol. 7, pp. 581-600.
68. K.O. Miller, J.F. Elliot, “Phase relationships in the systems Fe-Pb-Ni, Fe-Ni-C(Sat) and Fe-Pb-Ni-C; 1300° to 1550°C,” Transactions of the Metallurgical Society of AIME 218 (1960) 900-910.
69. B. Fleischer, J.F. Elliot, “The solubility of iron-nickel alloys in liquid lead: 700° to 1100°C.” In: Proceedings of the Physical Chemistry of metallic Solutions and Intermetallic Compounds (Symposium No. 9, paper 2F), 1958, June 4-6. National Physical Laboratory, London, UK; 1959, Vol. 1, pp. 2-12.
70. T. Alden, D.A. Stevenson, J. Wulff, “Solubility of nickel and chromium in molten lead,” Transactions of the Metallurgical Society of AIME 212 (1958) 1, 15-17.
71. E. Pelzel, “Die löslichkeit von kupfer, nickel und kobalt in flüssigem blei,” Metallurg 9 (1955) 692-694.
72. A.N. Morozov, Yu.A. Ageyev, “Solubility of lead in iron and iron alloys,” Russian Metallurgy 4 (1971) 78-81 (abridged translation).
73. W.M. Robertson, “Diffusion of cobalt and iron in liquid lead measured by grain boundary grooving,” Transactions of the Metallurgical Society of AIME 242 (1968) 10, 2139-2142.
74. H.U. Borgstedt, C. Guminski, “A model for the prediction of the corrosion of steels in flowing liquid lead alloys,” Journal of Nuclear Materials 303 (2002) 240-241.
75. G. Prévot, C. Cohen, J. Moulin, D. Schmaus, “Surface diffusion of Pb on Cu(110) at low coverage: competition between exchange and jump,” Surface Science 421 (1999) 364-376.

76. D.A. Skoog, F.J. Holler, S.R. Crouch, Principles of instrumental analysis, 6th ed. Belmont, USA: Brooks/Cole, Cengage Learning, 2006.
77. C.P. Wang, X.J. Liu, I. Ohnuma, R. Kainuma, K. Ishida, "Thermodynamic assessment of the Cu-Ni-Pb system," CALPHAD 24 (2000) 2, 149-167.
78. G. Ghosh, "Thermodynamic modeling of the nickel-lead-tin system," Metallurgical and Materials Transactions A 30A (1999) 1481-1494.
79. J. Niemelä, G. Effenberg, K. Hack, P.J. Spencer, "A thermodynamic evaluation of the copper – bismuth and copper – lead systems," CALPHAD 10 (1986) 1, 77-89.
80. O. Teppo, J. Niemelä, P. Taskinen, "The copper-lead phase diagram," Thermochimica Acta 185 (1991) 155-169.
81. B. Onderka, L.A. Zabdyr, "A new critical assessment of the copper-lead system," Scandinavian Journal of Metallurgy 30 (2001) 320-323.
82. B. Onderka, T. Pomianek, J. Romanowska, G. Wnuk, J. Wypartowicz, "Solubility of lead in liquid iron and the assessment of Fe-Pb system," Archives of Metallurgy and Materials 49 (2004) 1, 143 – 153.
83. N. David, "Modélisation thermodynamique du système (Al, Cu, Fe, In, Pb, Sn, Zn)," Doctoral thesis, l'Université Henri Poincaré, France, 2001.
84. M. Hämäläinen, R. Luoma, P. Taskinen, "Thermodynamic Analysis of the System Iron-Lead-Zinc," Helsinki University of Technology, Report TKK-V-B55, 1990.
85. G. Cacciamani, A. Dinsdale, M. Palumbo, A. Pasturel, "The Fe-Ni system: Thermodynamic modelling assisted by atomistic calculations," Intermetallics 18 (2010) 1148-1162.
86. G. Voss, "Die nickel-bleilegierungen," Zeitschrift für anorganische und allgemeine Chemie 57 (1908) 45-49.
87. T. Pomianek, "Thermodynamische eigenschaften des bleis in Ni-Pb-lösungen," Zeitschrift für Metallkunde 77 (1986) 6, 388-392.
88. H. Amenzou-Badrour, G. Moya, J. Bernardini, "Bulk diffusion and solubility of silver and nickel in lead, lead-silver and lead-nickel solid solutions," Acta Metallurgia 36 (1988) 3, 767-774.
89. D.A. Stevenson, J. Wulff, "Liquid-solid phase distribution studies in the systems iron-lead, cobalt-lead, chromium-tin, and nickel-silver," Transactions of the Metallurgical Society of AIME 221 (1961) 271-275.

90. I. Vaajamo, H. Johto, P. Taskinen, “A thermodynamic assessment of the Cu-Fe-Pb ternary system.” In: Proceedings of the European Metallurgical Conference (EMC) 2011, June 26-29, Düsseldorf, Germany. GDMB Medienverlag, Clausthal-Zellerfeld, Germany; 2011, Vol. 4, pp. 1283-1301.
91. E. Fromm, E. Gebhardt (Eds.), Gase und Kohlenstoff in Metallen. Reine und angewandte Metallkunde in Einzeldarstellungen, Bd. 26. Berlin-Heidelberg-New York: Springer-Verlag, 1976.
92. E. Raub, A. Engel, “Über rückläufige sättigungskurven bei der ausscheidung von mischkristallen aus der schmelze,” Zeitschrift für Metallkunde 37 (1946) 76-81.

Errata Corrige

Publication [I]

- Equation (1) should be "…+ IT^9" instead of "…+ IT^{-9}"
- On page 442 should be "…Al and Cu [32], as well as B and Cr [33]" instead of "…B and Cr [32], as well as Al and Cu [33]"
- Reference [20] should be "…undercooled…" instead of "…*u* dercooled…"
- Some of the values in Table 2 concerning the invariant reactions of system Ni-Pb were misprinted during publication. The values are corrected in Publication [IV] except for the values of Nash that are presented below.

Reaction	Reaction type	T/K	Compositions/x(Pb)			Author	Ref
L ↔ L1 + L2	Critical	1828		~ 0.29		Nash	[3]
L1 ↔ L2 + (Ni)	Monotectic	1613.15	0.1156	0.57	~ 0.01	Nash	[3]
L2 ↔ (Ni) + (Pb)	Eutectic	597.15	0.9954	~ 0.01	0.9983	Nash	[3]

Publication [II]

- On page 59 it should be "David [5]" instead of "Daniel [5]"
- In Table 3, concerning the invariant reactions of the Fe-Pb system, the critical reaction should be $L \leftrightarrow L_1 + L_2$, the monotectic reaction $L_1 \leftrightarrow L_2$ + bcc and the eutectic $L_2 \leftrightarrow$ bcc + fcc
- In Table 4, concerning the optimized thermodynamic parameters, the second parameter value 15699.12 J/mol·atom of Hämäläinen et al. is marked as temperature dependent (B_0) when it should be temperature independent (A_1).

Publication [IV]

- On page 69 it should be "LiF crystal" instead of "LIF-crystal"

Aalto-DD 173/2013

ISBN 978-952-60-5401-8
ISBN 978-952-60-5402-5 (pdf)
ISSN-L 1799-4934
ISSN 1799-4934
ISSN 1799-4942 (pdf)

Aalto University
School of Chemical Technology
Department of Materials Science and Engineering
www.aalto.fi

BUSINESS +
ECONOMY

ART +
DESIGN +
ARCHITECTURE

SCIENCE +
TECHNOLOGY

CROSSOVER

**DOCTORAL
DISSERTATIONS**